ORGANOMETALLICS

Article

pubs.acs.org/Organometallics

# Halide Control of *N,N*-Coordination versus *N,C*-Cyclometalation and Stereospecific Phenyl Ring Deuteration of Osmium(II) *p*-Cymene Phenylazobenzothiazole Complexes

Russell J. Needham,[†] Abraha Habtemariam,[†] Nicolas P. E. Barry,[†,‡] Guy Clarkson,[†] and Peter J. Sadler*[,†]

[†]Department of Chemistry, University of Warwick, Gibbet Hill Road, Coventry CV4 7AL, U.K.

[‡]School of Chemistry and Biosciences, University of Bradford, Bradford BD7 1DP, U.K.

Supporting Information

**ABSTRACT:** We report the synthesis of halido Os(II) *p*-cymene complexes bearing bidentate chelating phenylazobenzothiazole (AZBTZ) ligands. Unlike the analogous phenylazopyridine (AZPY) complexes, AZBTZ-$NMe_2$ is capable of both *N,N*-coordination to Os(II) and cyclometalation to form *N,C*-coordinated species. *N,C*-Coordination occurs via an azo nitrogen and an ortho carbon on the aniline ring, as identified by $^1$H NMR and X-ray crystallography of [Os(*p*-cym)(*N,N*-AZBTZ-$NMe_2$)Cl]$PF_6$ (**1a**), [Os(*p*-cym)(*N,N*-AZBTZ-$NMe_2$)Br]$PF_6$ (**2a**), [Os(*p*-cym)(*N,C*-AZBTZ-$NMe_2$)Br] (**2b**), and [Os(*p*-cym)(*N,C*-AZBTZ-$NMe_2$)I] (**3b**). The *N,C*-coordinated species is more stable and is not readily converted to the *N,N*-coordinated complex. Analysis of the crystal structures suggests that their formation is influenced by steric interactions between the *p*-cym and AZBTZ-$NMe_2$ ligands: in particular, larger monodentate halide ligands favor *N,C*-coordination. The complexes [Os(*p*-cym)(*N,N*-$Me_2$-AZBTZ-$NH_2$)Cl]$PF_6$ (**4**) and [Os(*p*-cym)(*N,N*-$Me_2$-AZBTZ-$NH_2$)I]$PF_6$ (**5**) were synthesized with methyl groups blocking the ortho positions on the aniline ring, forcing an *N,N*-coordination geometry. $^1$H NMR NOE experiments confirmed hindered rotation of the arene ligand and steric crowding around the metal center. Complex **2b** exhibited unexpected behavior under acidic conditions, involving regiospecific deuteration of the aniline ring at the meta position, as observed by $^1$H NMR and high-resolution ESI-MS. Deuterium exchange occurs only under acidic conditions, suggesting an associative mechanism. The calculated partial charges on **2b** show that the meta carbon is significantly more negatively charged, which may account for the regiospecificity of deuterium exchange.

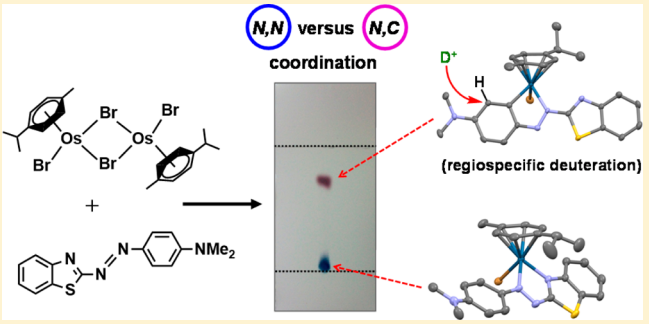


## INTRODUCTION

There is growing interest in the chemistry of organometallic osmium complexes, with potential applications in a range of areas, including catalysis[1−4] and anticancer activity.[5−9] For example, osmium(II) arene complexes containing *N,N*-chelating phenylazopyridine (AZPY) ligands exhibit promising anticancer properties and novel mechanisms of action.[10−14] Here we explore Os(II) complexes with phenylazobenzothiazole (AZBTZ) ligands. Interestingly, AZBTZs have established applications in the field of dyes and pigments owing to their intense red coloration.[15] They can also be utilized as probes for *in vivo* radioimaging of neurofibrillary tangles in Alzheimer's diseased brains and show promising selective binding toward $\beta$-amyloid peptides and hyper-phosphorylated $\tau$ proteins associated with Alzheimer's disease.[16]

AZBTZs are analogous to AZPY ligands, the pyridine being substituted by a benzothiazole unit. Benzothiazole is a bicyclic ring system consisting of a benzene ring fused to a five-membered 1,3-thiazole ring. Because of their pronounced biological and pharmacological activities, AZBTZ derivatives are of great interest for medicinal applications. Numerous organic benzothiazole compounds have been reported to have promising anticancer activity,[17−20] suggesting that Os(II) complexes containing benzothiazole groups may possess potential as anticancer agents. Indeed, there are studies highlighting organometallic complexes bearing benzothiazole groups with antiproliferative activity,[21,22] and DNA binding capabilities.[23] Most notable are Os(II) and Ru(II) complexes reported by Keppler *et al.* as benzothiazole and benzimidazole pharmacophoric inhibitors of protein kinases.[22]

AZBTZs contain functionalities with metal coordination affinity. In our present study we synthesized two types of complexes (see Chart 1); charged *N,N*-coordinated complexes, [Os(*p*-cym)(*N,N*-{$R^A$}$_2$-AZBTZ-N{$R^B$}$_2$)X]$PF_6$, and neutral *C,N*-coordinated complexes, [s(*p*-cym)(*N,C*-AZBTZ-$NMe_2$)X] where *p*-cym = *p*-cymene, $R^A$, $R^B$ = H, Me, and X = Cl, Br, I. We have determined their single-crystal X-ray crystal structures,

**Received:** July 13, 2017
**Published:** November 9, 2017

  

DOI: 10.1021/acs.organomet.7b00501
*Organometallics* 2017, 36, 4367−4375

**Chart 1. Os(II) Complexes Formed from Ligands L and L*[d]**

(A)

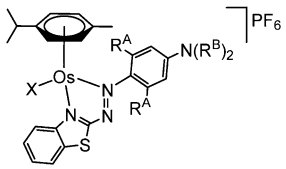

| Complex | X | $R^A$ | $R^B$ |
|---|---|---|---|
| **1a**[a] | Cl | H | Me |
| **2a**[a] | Br | H | Me |
| **3a**[c] | I | H | Me |
| **4**[b] | Cl | Me | H |
| **5**[b] | I | Me | H |

(B)

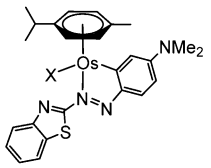

| Complex | X |
|---|---|
| **1b**[b] | Cl |
| **2b**[a] | Br |
| **3b**[a] | I |

[a]Product isolated and X-ray structure determined. [b]Product isolated. [c]Product observed in the reaction mixture by $^1$H NMR but not isolated. [d]Complexes **1**–**3** with **L** and complexes **4** and **5** with **L***. Complexes **1a**–**3a**, **4**, and **5** are *N,N*-coordinated species, and **1b**–**3b** are *N,C*-coordinated complexes.

stability in aqueous media and discovered unusual properties of *N,C*-coordinated species, including stereospecific phenyl ring deuteration.

## RESULTS

**Synthesis of AZBTZ Ligands.** The bidentate phenylazobenzothiazole ligand AZBTZ-$NMe_2$ (**L**) was synthesized via a diazotization coupling reaction (Scheme S1 in the Supporting Information).[15] Nitrosation of the primary amine in 2-aminobenzothiazole occurs when the nitrosonium cation is generated *in situ* from sodium nitrite and sulfuric acid, leading to the formation of a reactive diazonium salt intermediate. On addition of *N,N*-dimethylaniline, the electrophilic diazonium salt reacts at the para position of the aniline ring to form the highly colored ligand **L**. Reactivity at the ortho position of the ring is blocked by the presence of tertiary amine methyl groups. Similarly, a second ligand, $(Me)_2$-AZBTZ-$NH_2$ (**L***), was synthesized via the same reaction. When a diazonium salt was formed from 3,5-dimethylaniline, there were no methyl groups situated on the amine group to prevent ortho-electrophilic addition. An ortho-substituated impurity was found at 18% by $^1$H NMR, and the product was purified by silica column chromatography.

**Synthesis of Os(II) Arene AZBTZ Complexes.** Os(II) arene AZBTZ complexes were synthesized by stirring 2 mol equiv of **L** with an Os(II) *p*-cym dimer, $[Os(\eta^6\text{-}p\text{-cym})X_2]_2$ (where X = Cl, Br, I), in EtOH at ambient temperature. All three dimers reacted with **L** to form a positively charged *N,N*-coordinated complex, **A**, and a neutral cyclo-metalated *N,C*-coordinated complex, **B**, in varying ratios (Scheme 1). These were observed in reaction mixtures via silica thin-layer chromatography (TLC) using MeOH as eluent. Positively charged *N,N*-complexes exhibit strong affinities for silica and do not travel far from the TLC plate baseline. In contrast, neutral *N,C*-complexes travel with the mobile phase with $R_f$ values ranging between 0.70 and 0.74.

The percentages of **A** (*N,N*) and **B** (*N,C*) complexes formed were determined for each dimer from $^1$H NMR spectra of the reaction mixtures after 18 h of stirring, by measuring the integrals of aliphatic *p*-cym $CH_3$ doublets (Figure S1 in the Supporting Information). For *N,N*-coordinated complexes, these doublets lie significantly closer to one another (0.09–0.11 ppm apart), in comparison to *N,C*-coordinated complexes (0.25–0.30 ppm apart). When X = Cl, Br, both the charged complexes **1a** and **2a** and neutral complexes **1b** and **2b** were isolated (Chart 1). However, when X = I, only the neutral complex **3b** was isolated as the major product. Complexes **1b**–**3b** can be easily purified via silica flash column chromatography, which was not possible for charged complexes **1a** and **2a** due to their high affinities for silica.

The reaction conditions were modified with the intention of favoring *N,N*- over *N,C*-coordination. When the reaction between $[Os(\eta^6\text{-}p\text{-cym})I_2]_2$ and **L** was carried out in the aprotic and weakly coordinating solvent DCM, formation of the *N,N*-coordinated species **3a** was still disfavored. Furthermore, carrying out the reaction between $[Os(\eta^6\text{-}p\text{-cym})Br_2]_2$ and **L** in the presence of HBr did not prevent deprotonation of the phenyl ring and hence prevent formation of the *N,C*-coordinated species. Ligand **L*** has methyl groups situated on the aniline ring ortho to the azo bond ($R^A$, Chart 1), hindering cyclometalation and formation of an *N,C*-coordinated species. When $[Os(\eta^6\text{-}p\text{-cym})I_2]_2$ was reacted with 2 mol equiv of **L*** the reaction took notably longer for the initial color change to occur but was successful in yielding complex **5**. Complex **4** was

**Scheme 1. Synthetic Route to Charged *N,N*-Coordinated Complexes, A, and Neutral *N,C*-Coordinated Complexes, B**

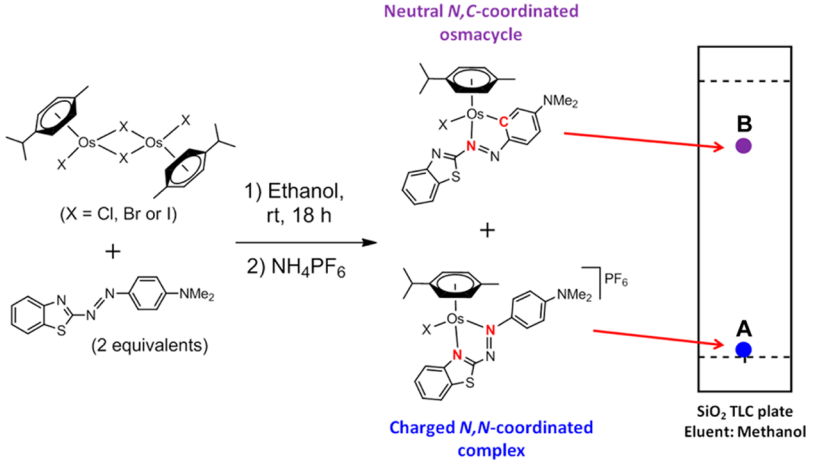




DOI: 10.1021/acs.organomet.7b00501
*Organometallics* 2017, 36, 4367–4375

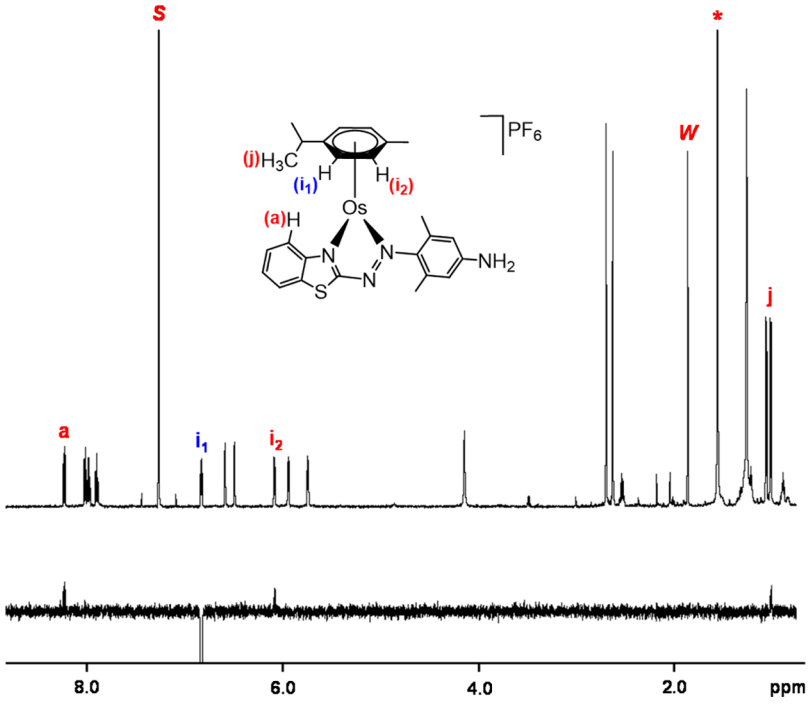


**Figure 1.** (A) 600 MHz $^1$H NMR spectrum of **5** in chloroform-$d_1$. (B) The corresponding $^1$H-selective NOE spectrum. The deshielded proton at 6.84 ppm, $i_1$, was irradiated. Protons close (ca. <4 Å) are labeled. The residual solvent peak (*S*), residual water peak (*W*), and the impurity in the chloroform-$d_1$ solvent (*) are highlighted. The iodido monodentate ligand is pointing into the plane of the page for clarity.

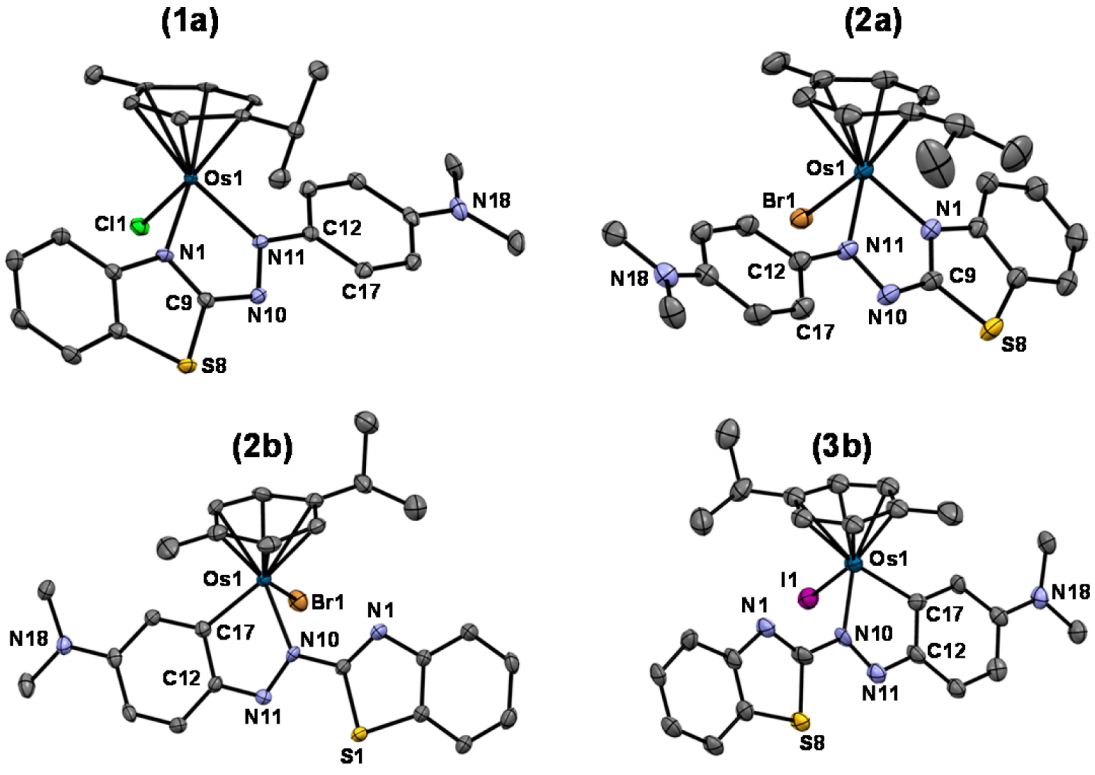


**Figure 2.** ORTEP diagrams of complexes **1a**, **2a**, **2b**·0.5$C_3H_6O$, and **3b**·0.5$CHCl_3$. Ellipsoids are shown at the 50% probability level, and all hydrogens, counterions, and solvent molecules have been omitted for clarity.

also synthesized via the same reaction using $[Os(\eta^6\text{-}p\text{-cym})Cl_2]_2$.

**Characterization of Complexes.** The aromatic region of the $^1$H NMR spectrum of **1a** (Figure S2 in the Supporting Information) shows 12 aromatic protons. In contrast, the $^1$H NMR spectrum of complex **3b** reveals a species containing only 11 aromatic protons (Figure S3 in the Supporting Information). We confirmed that the missing proton is from the 3-position of the aniline ring, which is bonded to Os(II) to form a neutral complex. This structure is characterized by a doublet of



DOI: 10.1021/acs.organomet.7b00501
*Organometallics* 2017, 36, 4367−4375

Table 1. Selected Bond Lengths (Å), Interatomic Distances (Å), and Bond/Torsion Angles (deg), Observed in the X-ray Crystal Structures of Complexes 1, 2a, 2b·0.5$C_3H_6O$, and 3b·0.5$CHCl_3$ (X = Cl, Br, I)

| | 1a | 2a | 2b·0.5$C_3H_6O$ | 3b·0.5$CHCl_3$ |
|---|---|---|---|---|
| | | Bond Lengths (Å) | | |
| Os1−X1 | 2.3784(6) | 2.5242(3) | 2.5532(8) | 2.7078(9) |
| Os1−N1 | 2.072(2) | 2.053(2) | N/A | N/A |
| Os1−N10 | N/A | N/A | 2.074(5) | 2.079(8) |
| Os1−N11 | 2.079(2) | 2.088(2) | N/A | N/A |
| Os1−C17 | N/A | N/A | 2.020(7) | 2.050(11) |
| N10−N11 | 1.334(3) | 1.335(3) | 1.324(8) | 1.316(13) |
| Os1−arene centroid | 1.705 | 1.706 | 1.722 | 1.721 |
| | | Distances (Å) | | |
| H3···H24 | 2.237 | 2.380 | N/A | N/A |
| H13···H22 | 2.270 | 2.232 | N/A | N/A |
| H16···H22/H24 | N/A | N/A | 2.441 | 2.274 |
| S1/S8···S1/S8 | N/A | N/A | 3.229 | 3.249 |
| | | Bond Angles (deg) | | |
| $\theta_{X1-Os1-N1}$ | 84.56(7) | 85.74(6) | N/A | N/A |
| $\theta_{N1-Os1-N11}$ | 75.01(9) | 74.60(8) | N/A | N/A |
| $\theta_{N11-Os1-X1}$ | 85.55(6) | 85.97(6) | N/A | N/A |
| $\theta_{X1-Os1-N10}$ | N/A | N/A | 84.87(16) | 85.2(3) |
| $\theta_{N10-Os1-C17}$ | N/A | N/A | 75.8(2) | 75.8(4) |
| $\theta_{C17-Os1-X1}$ | N/A | N/A | 86.2(2) | 85.7(3) |
| | | Torsion Angles (deg) | | |
| $\theta_{N1-C9-N10-N11}$ | −1.52 | 0.72 | N/A | N/A |
| $\theta_{N10-N11-C12-C17}$ | −17.66 | 14.40 | 1.06 | 0.44 |
| $\theta_{S1/S8-C9-N10-N11}$ | N/A | N/A | 0.39 | −3.29 |

doublets assignable to proton *g* ($J$ = 9.2, 2.5 Hz), which has short-range coupling to proton *h* ($^3J$ = 9.2 Hz) and long-range coupling to proton *f* ($^4J$ = 2.5 Hz). The $^1$H NMR spectrum of complex **5** consists of 10 aromatic protons, 4 of which correspond to the *p*-cym ligand. One *p*-cym aromatic doublet at 6.82 ppm is considerably more deshielded than the others between 6.09 and 5.72 ppm. A selective $^1$H NMR NOE experiment was conducted to identify proximate protons (Figure 1). The deshielded arene proton $i_1$ is close to another aromatic *p*-cym proton $i_2$, a methyl group on the arene *j*, and interestingly, close to the proton at the 8-position on the benzothiazole group, *a*. In comparison, the chlorido complex **4** also shows the same trend with a deshielded *p*-cym proton residing at 6.90 ppm.

ESI-MS analysis of the charged *N,N*-coordinated complexes **1a**−**3a**, **4**, and **5** revealed *m*/*z* peaks that correspond to the cationic species without their counteranion, [M − $PF_6$]. Alternatively, neutral *N,C*-coordinated complexes **1b**−**3b** were observed as species with either a $H^+$ or $Na^+$ cation, [M + $H^+$] or [M + $Na^+$].

**X-ray Crystallography.** The structures of complexes **1a** and **2a**−**3b** were determined by single-crystal X-ray diffraction (Figure 2). The crystallographic data are shown in Table S1 in the Supporting Information, and selected bond lengths, bond angles, torsion angles, and interatomic distances are summarized in Table 1. The complexes adopt the familiar pseudo-octahedral three-legged piano-stool geometry that is common for Os(II) $\eta^6$-arene structures, with Os(II) $\pi$-bonded to the *p*-cym ligand. Osmium(II) is also coordinated to a monodentate halide ligand and the bidentate ligand **L** via either *N,N* or *N,C* atoms, which constitute the three legs of the piano stool. All complexes exhibit a five-membered chelate ring with **L**: N1−C9−N10−N11−Os1 for **1a** and **2a** and N10−N11−C12−C17−Os1 for **2b** and **3b**. They all crystallize as racemates owing to the presence of a chiral Os(II) center. Complexes **1a** and **2a** have $PF_6^-$ counterions in their X-ray crystal structures, whereas complexes **2b** and **3b** incorporate molecules of acetone and chloroform in their crystal lattice, respectively, at a 2:1 ratio of complex to solvent.

The X-ray crystal structures of *N,N*-coordinated complexes **1a** and **2a** confirm that ligand **L** is bound to Os(II) via the N atom of the benzothiazole group and N1 or N11 of the azo bond. Weak $\pi-\pi$ interactions between aniline rings (3.46 Å, centroid to centroid) were observed for **1a** (Figure S4 in the Supporting Information). Short H···H distances were observed between aromatic hydrogens on the *p*-cym ligand and bidentate ligand **L**; H13···H22 and H3···H24 for complexes **1a** and **2a**. The torsion angle $\theta_{N1-C9-N10-N11}$ serves as a measure of distortion of the chelate ring from planarity, and values of −1.52 and 0.72° were calculated, respectively, for complexes **1a** and **2a**. The torsion angle $\theta_{N10-N11-C12-C17}$ describes the angle between the chelate ring and the aniline ring. With values of −17.66 and 14.40° for **1a** and **2a**, respectively, ligand **L** is not aligned flat within the structure. In contrast, *N,C*-coordinated complexes **2b** and **3b** exhibit fewer H···H clashes between the *p*-cym ligand and ligand **L** (H16···H22/H24). The torsion angle $\theta_{S1/S8-C9-N10-N11}$, which serves as the angle between the chelate ring and the benzothiazole moiety for complexes **2b** and **3b**, is small (0.39 and −3.29°, respectively). This results in a closely planar ligand **L** within the crystal structures. The torsion angles serve as a measure of distortion of the chelate ring from planarity for **2b** and **3b** ($\theta_{N10-N11-C12-C17}$), and are 1.06 and 0.44°, respectively. Also observed in **2b** and **3b** are intermolecular S···S contacts, mediated through the free and uncoordinated benzothiazole groups with outwardly pointing S atoms (Figure S4 in the Supporting Information).

**Aqueous Solubility and Stability.** All synthesized complexes were too insoluble in aqueous media for biological



DOI: 10.1021/acs.organomet.7b00501
Organometallics 2017, 36, 4367−4375

studies and stability testing in $D_2O$ by $^1H$ NMR. The stabilities of **1a,b** in MeOH/$H_2O$ (1/1, v/v) were monitored over a 24 h period by UV−vis spectroscopy at 25 °C. Changes in the UV−vis absorption spectrum of **1a** were monitored over 24 h, and decreases in intensity of the bands at 653 and 716 nm were noted (Figure S5 in the Supporting Information). The presence of 100 mM NaCl inhibited spectral changes over 24 h. In contrast, no decomposition of **1b** was observed over 24 h in MeOH/$H_2O$ (1/1, v/v), with two stable maxima observed at 447 and 562 nm.

**Acid Stability and Regiospecific Aniline Ring Deuteration.** When complex **2b** was stirred with 100 mol equiv of HBr in MeOH, no conversion to the *N,N*-coordinated species **2a** was observed by $^1H$ NMR (HBr was used as the acid to avoid halide substitution on the metal). It was only after heating under reflux for 2 days that a new set of small aliphatic *p*-cym proton peaks began to emerge in the $^1H$ NMR spectrum (Figure S6 in the Supporting Information). TLC analysis in MeOH revealed a small blue spot residing close to the baseline, suggesting the presence of a charged *N,N*-coordinated species. A solution of complex **2b** with 3 mol equiv of HBr in methanol-$d_4$ was studied by $^1H$ NMR. The peak for the aromatic hydrogen neighboring the Os−C bond ($H_a$, 7.58 ppm) disappeared almost completely after 15 h at 25 °C. Its disappearance coincided with a loss of long-range proton coupling to $H_b$ ($^4J$ = 2.5 Hz, 7.26 ppm; see Figure 3). The

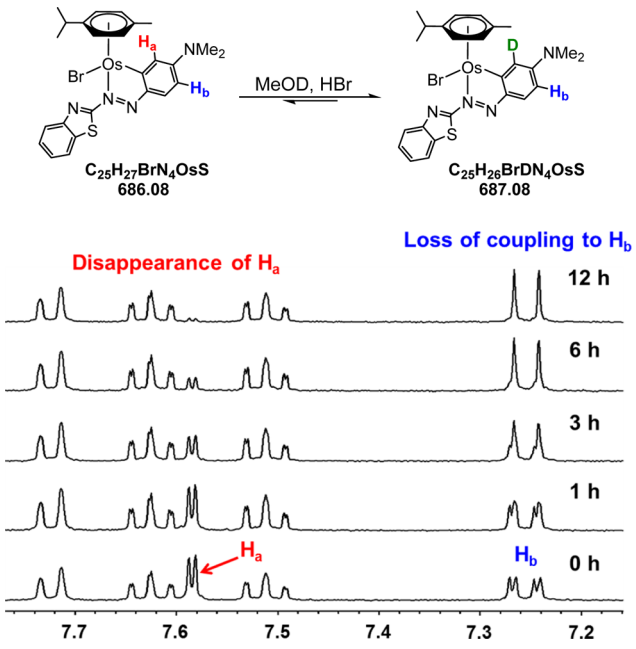


**Figure 3.** 400 MHz $^1H$ NMR spectra of complex **2b** (aromatic region) with 3 mol equiv of HBr in methanol-$d_4$. The disappearance of proton $H_a$ (7.58 ppm) is accompanied by loss of long-range coupling between protons $H_b$ and $H_a$ ($^4J$ = 2.5 Hz).

substitution of protium at this position with deuterium occurs only in the presence of an acid. High-resolution mass spectrometry of the NMR sample in methanol-$d_4$ revealed the presence of the deuterated complex, showing exact masses of *m/z* 688.0876 and 710.0696, which correspond to the formulas $[C_{25}H_{26}BrDN_4OsS + H^+]$ and $[C_{25}H_{26}BrDN_4OsS + Na^+]$, respectively (see Figure S7 in the Supporting Information). A kinetic $^1H$ NMR study was conducted at 25 °C, and a spectrum was collected every 30 min to observe the disappearance of $H_a$ (measured by integration). The reaction exhibits first-order kinetics for deuteration of the phenyl ring with a rate constant of $6.91 \times 10^{-5}$ $s^{-1}$ and a half-life of $1.00 \times 10^4$ s (Figure S8 in the Supporting Information).

**Mulliken Partial Charges.** Mulliken partial charge calculations of complex **2b** are shown in Figure S9 in the Supporting Information. Carbon C1 is significantly more negatively charged than the other carbon atoms making up the aniline ring. Furthermore, the aniline ring exhibits disrupted aromaticity with only two C═C bonds present, C1═C2 and C4═C5, which have calculated bond lengths of 1.384 and 1.363 Å, respectively. These are consistent with the X-ray crystal structure, which has bond lengths of 1.386(9) and 1.351(9) Å, respectively. In contrast, the bond lengths of singly bonded C2−C3 and C5−C6 are 1.478 and 1.470 Å, respectively, in the calculated structure and 1.434(9) and 1.433(10) Å in the crystal structure. The calculation also shows that $CH_3$ carbons have significantly high negative charges.

## DISCUSSION

**Intramolecular C−H Bond Activation and Cyclometalation.** Reactions between Os(II) *p*-cym dimers and **L** were expected to yield *N,N*-coordinated cationic species, analogous to AZPY complexes reported previously.[10,11] To our surprise, mixtures containing both *N,N*- and *N,C*-coordinated complexes were obtained. Formation of the *N,C*-cyclometalated complex requires C−H bond activation, a challenging step involving deprotonation of the aniline ring at the ortho position. There are numerous examples of ruthenium, rhodium, osmium, and iridium complexes formed via direct arylation of ligands such as 2-phenyl-substituted pyridines.[24−28] Metalation of the phenyl ring invariably occurs at the ortho position and results in five-membered chelate rings. Older synthetic routes utilize a transmetalation pathway involving ortho-mercurated species, eliminating the need for C−H activation.[29−32] However, direct metalation of 2-phenylpyridine (2-PhPy) is also possible in the presence of bases such as acetate and is directed by the nitrogen-containing pyridine moiety, which initially binds to the metal center. In the reaction between $[Os(\eta^6\text{-}p\text{-cym})X_2]_2$ and **L**, the direction may be guided via initial coordination to the azo bond nitrogen, and C−H activation occurs spontaneously and remarkably in the absence of an additional base. Cerón-Camacho *et al.* have reported the successful electrophilic cyclo-osmation of the bidentate ligands 2-PhPy and *N,N*-dimethylbenzylamine,[33] the latter of which was also achieved in the absence of a base. The ligand is believed to act as both a substrate and a base for its own C−H bond cleavage. Similar to the case for *N,N*-dimethylbenzylamine, **L** possesses a basic amine group that could be responsible for assisting C−H bond cleavage at the ortho position of the aniline. A review of the literature suggests that a likely mechanism may involve base-assisted $S_E3$ electrophilic cyclometalation.[34,35] Alternatively, a mechanism involving an agostic ortho Os(C−H) bond might be possible (see Scheme S2 in the Supporting Information).[35,36] Both mechanisms require the nucleophilic $-NMe_2$ group on **L** to play a role as a proton acceptor during C−H bond activation. Such mechanisms have been proposed for the cyclometalation of 2-PhPy with ruthenium $\eta^6$-arene complexes.

**Selectivity toward *N,C*-Complex Formation over *N,N*-Coordination.** It was initially anticipated that ligand **L** may coordinate to the metal via the S atom of the benzothiazole group. However, to the best of our knowledge, there are no


DOI: 10.1021/acs.organomet.7b00501
*Organometallics* 2017, 36, 4367−4375

literature reports of benzothiazoles coordinating to metal centers through the S atom.[37] The benzothiazole group of **L** favors N-binding in our complexes, as confirmed by the X-ray crystal structures of complexes **1a** and **2a**. *N,C*-Coordination is preferred when X = Br, I, but for X = Cl, *N,N*-coordination is preferred. From crystallographic observations, it is most likely that the ratio of products formed is influenced by steric considerations. Assessment of the crystal structures shows that the *N,N*-coordinated species **1a** and **2a** exhibit more steric hindrance in the form of H···H clashes between *p*-cym and **L** than do *N,C*-coordinated species **2b** and **3b**. *N,N*-Coordinated species also show greater torsion angles in ligand **L** in comparison to *N,C*-coordinated species, where **L** is close to planar. The ligand **L** in **1a** and **2a** appears to show aniline ring twisting to reduce clashing with the *p*-cym ligand. It is most likely that when X = Br, I, *N,N*-coordination is more difficult owing to the increased halide size, hence producing greater steric crowding around the metal center, which pushes the organic ligands closer together. Increased steric crowding may promote coordination via the cyclometalation route (Figure 4).

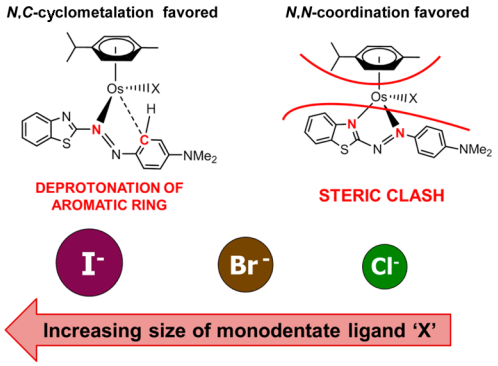


**Figure 4.** Diagram illustrating the possible influence of steric effects on the ratios of products formed when $[Os(\eta^6\text{-}p\text{-cym})X_2]_2$ reacts with **L**. *N,N*-Coordination results in steric clashes between *p*-cym and **L** and is less favored when the monodentate ligand is large. *N,C*-Coordination is preferred, relieves steric tension, and involves spontaneous deprotonation of the aromatic ring.

Preferential binding via cyclometalation may also be influenced by the weaker binding of benzothiazole in comparison to pyridine. The complex **FY026**, $[Os(p\text{-cym})(AZPY\text{-}NMe_2)I]PF_6$, synthesized previously contains an phenylazopyridine ligand analogous to **L** with distinct *N,N*-coordination.[11] Pyridine is a stronger $\pi$-acceptor moiety than benzothiazole. Both pyridine and benzothiazole are weak $\sigma$-donors, but the reduced $\pi$-acceptor capability of benzothiazole may also influence preferential *N,C*-coordination, as well as steric factors.

**Stability in Aqueous Media.** Our UV−vis studies in aqueous media showed that *N,N*-coordinated complex **1a** underwent a chemical change over a 24 h period that was prevented in the presence of NaCl (100 mM), indicating that loss of the chloride ligand is involved. In contrast, *N,C*-coordinated complex **1b** showed no sign of decomposition over 24 h and exhibited a very stable Os−Cl bond.

**Hindered Arene Rotation in 5.** A $^1$H-selective NOE study confirmed that the observed deshielded aromatic *p*-cym proton in $[Os(p\text{-cym})(N,N\text{-}Me_2\text{-}AZBTZ\text{-}NH_2)I]PF_6$ (**5**) is in close proximity with an aromatic proton belonging to coordinated **L***. The steric crowding is likely to be as a result of *N,N*-coordination, which in this case is forced due to blocking of the ortho positions on the aniline ring, preventing cyclometalation from occurring. *N,N*-Coordinated structures containing **L**, **1a** and **2a**, do not exhibit the same trend. It is therefore likely that hindered rotation may also play a role in the deshielding of the observed proton. The methyl groups at positions $R^A$ in complexes **4** and **5** (Chart 1) may play a role in hindering rotation of the *p*-cym ligand.

**Regiospecific Aniline Ring Deuteration of Complex 2b.** Remarkably, $[Os(p\text{-cym})(N,C\text{-}AZBTZ\text{-}NMe_2)Br]$ (**2b**) undergoes deuteration of the aniline ring at a position ortho to the Os−C bond (meta $H_a$), but only in the presence of acid (HBr). On addition of 3 mol equiv of HBr, the $^1$H NMR signal of $H_a$ disappeared along with its coupling to $H_b$, following first-order kinetics. The Mulliken partial charge calculation shows that the carbon where deuteration occurs carries a greater negative partial charge (−0.461) in comparison to the other CH carbons making up the aniline ring (−0.264 and −0.275). Interestingly, its exchange with deuterium occurred under acidic conditions, suggesting an associative mechanism of exchange (see Scheme S3 in the Supporting Information).

## CONCLUSIONS

We report the synthesis of novel Os(II) *p*-cym phenylazobenzothiazole complexes in which the chelated ligand can adopt two coordination modes: *N,N*- or *N,C*-coordination. The crystallographic data suggest that *N,N*-coordination leads to steric crowding around the metal and so is formed as a minor product when the monodentate halide ligand is large (X = I, Br). *N,C*-Coordination requires C−H bond activation for carbon metalation and occurs spontaneously in the absence of a base, most likely owing to the presence of the basic $NMe_2$ substituent, which assists deprotonation of the aromatic ring. The mechanism of cyclometalation is not clear but may occur via an $S_E3$ mechanism. Furthermore, the *N,N*-coordinated species **1a** was unstable in aqueous media over 24 h but stable over 24 h in the presence of 100 mM NaCl, indicating that the decomposition of **1a** involves loss of the monodentate ligand and possible hydrolysis. In contrast, the *N,C*-coordinated analogue **2b** was stable over 24 h.

*N,N*-Coordination in complexes **4** and **5** was promoted by intentional blocking of the C−H activation sites with methyl groups. This led to complexes with an unusually deshielded aromatic *p*-cym $^1$H NMR resonance. In selective $^1$H NMR NOE studies, the deshielded proton in **5** was observed in close proximity to a proton on the benzothiazole group, thus providing further evidence of steric crowding in the *N,N*-coordinated complexes.

The *N,C*-coordinated complex **2b** exhibited unusual behavior. In the presence of acid (HBr) in methanol-$d_4$, the ortho H (neighboring the Os−C bond) exchanges with deuterium with a half-life of 2.8 h at 25 °C. Calculations of the Mulliken partial charges showed an increased partial negative charge on the ortho C, consistent with an associative mechanism of exchange.

## EXPERIMENTAL SECTION

**Materials.** $OsCl_3 \cdot 3H_2O$ was purchased from Sigma-Aldrich (UK) and Heraeus (South Africa). $\alpha$-Terpinene, ammonium hexafluorophosphate, and hydrobromic acid were purchased from Sigma-Aldrich (UK). *N,N*-Dimethylaniline, 3,5-dimethylaniline, 2-aminobenzothiazole, sodium nitrite, sulfuric acid (>95%), and glacial acetic acid were purchased from Fisher Scientific (UK). All organic solvents



DOI: 10.1021/acs.organomet.7b00501
Organometallics 2017, 36, 4367−4375

were purchased from commercial suppliers and used as received. The dimers $[Os(p\text{-cym})X_2]_2$, where X = Cl, Br, I, were prepared according to literature procedures.[38−40]

**Syntheses.** *Synthesis of Ligands.* The synthesis of ligands **L** and **L*** was performed by the following procedure. 2-Aminobenzothiazole (500.0 mg, 3.33 mmol) was mixed with glacial acetic acid (20 mL) and cooled to 0 °C in a water/ice bath. Sulfuric acid (>95%, 7 mL) was then added. A solution of $NaNO_2$ (252.7 mg, 3.66 mmol) in deionized water (10 mL) was added dropwise to the stirred mixture, and it instantaneously turned yellow-orange. The mixture was stirred for 2 h at 0 °C. An ice-cold solution of *N,N*-dimethylaniline (for **L**, 3.33 mmol) or 3,5-dimethylaniline (for **L***, 3.33 mmol) in MeOH (34 mL) was added dropwise, and the mixture turned dark purple. The mixture was stirred for a further 18 h, was warmed to ambient temperature, and then was combined with water (200 mL) and DCM (100 mL), and the layers were separated. The aqueous layer was washed with DCM (2 × 50 mL), and the combined DCM extracts were washed with water (2 × 50 mL), dried over $MgSO_4$, and filtered; the solvent was removed under reduced pressure, yielding a dark precipitate. The crude product was recrystallized from a minimum amount of chloroform, giving a dark green precipitate. The product was collected by filtration, washed with ice-cold $Et_2O$ (2 × 5 mL), and dried overnight in a vacuum desiccator. Characterization data are shown in the Supporting Information.

*Synthesis of [Os(η⁶-p-cym)(N,N-AZBTZ-NMe₂)Cl]PF₆ (**1a**).* $[Os(\eta^6\text{-}p\text{-cym})Cl_2]_2$ (50.0 mg, 63.2 μmol) and 4-(2-benzothiazolylazo)-*N,N*-dimethylaniline (37.5 mg, 132.8 μmol) were dissolved in EtOH (20 mL). The mixture was stirred at 50 °C for 2 h, and the color changed to dark blue. The mixture was stirred for 18 h at ambient temperature, and $NH_4PF_6$ (103.1 mg, 0.63 mmol) was added. The volume was reduced under reduced pressure to ∼2 mL, and the mixture was placed in a freezer overnight. The resulting dark blue precipitate was collected by filtration. The precipitate was dissolved in chloroform (10 mL), stirred for 1 h, and filtered. The filtrate was collected, and the solvent was removed under reduced pressure. The resulting dark blue precipitate was recrystallized from a minimum amount of EtOH and placed in a freezer (−20 °C) overnight. The product was collected by filtration and washed with ice-cold EtOH (2 × 1 mL) and $Et_2O$ (2 × 5 mL). The product was dried overnight in a vacuum desiccator. Yield: 44.9 mg (45%).

*Synthesis of [Os(η⁶-p-cym)(N,C-AZBTZ-NMe₂)Cl] (**1b**).* $[Os(\eta^6\text{-}p\text{-cym})Cl_2]_2$ (50.0 mg, 63.2 μmol) and 4-(2-benzothiazolylazo)-*N,N*-dimethylaniline (37.5 mg, 132.8 μmol) were dissolved in EtOH (20 mL). The mixture was stirred at 50 °C for 2 h, and the color changed to dark blue. The mixture was stirred for 18 h at ambient temperature, and then the solvent was removed under reduced pressure. The product was purified via flash column chromatography ($SiO_2$, 50/1 DCM/MeOH, $R_f$ = 0.34). The selected fractions containing the product were combined, and the solvent was removed under reduced pressure to give a dark purple precipitate. The precipitate was recrystallized from a minimum amount of EtOH and placed in a freezer (−20 °C) overnight. The product was collected by filtration, washed with ice-cold EtOH (2 × 1 mL) and $Et_2O$ (2 × 5 mL), and then dried in a vacuum desiccator overnight. Yield: 14.9 mg (18%).

*Synthesis of [Os(η⁶-p-cym)(N,N-AZBTZ-NMe₂)Br]PF₆ (**2a**) and [Os(η⁶-p-cym)(N,C-AZBTZ-NMe₂)Br] (**2b**).* $[Os(\eta^6\text{-}p\text{-cym})Br_2]_2$ (70.0 mg, 72.3 μmol) and 4-(2-benzothiazolylazo)-*N,N*-dimethylaniline (40.8 mg, 144.6 μmol) were dissolved in EtOH (20 mL). The mixture was stirred at 50 °C for 2 h, and the color changed to dark blue-purple. The mixture was stirred for 18 h at ambient temperature, and $NH_4PF_6$ (103.1 mg, 0.63 mmol) was added. The solvent was removed under reduced pressure, and the dark blue residue was redissolved in chloroform (20 mL) and stirred for 1 h. The mixture was filtered, giving a precipitate predominantly containing **2b** and a filtrate predominantly containing **2a**.

For **2a**, the filtrate was concentrated under reduced pressure to ∼1−2 mL, combined with a small amount of $Et_2O$ (<1 mL), and placed in a freezer (−20 °C) overnight. The resulting dark blue precipitate was collected by filtration, washed with ice-cold EtOH (1 mL) and $Et_2O$ (2 × 5 mL), and dried overnight in a vacuum desiccator. Yield: 9.9 mg (8%).

For **2b**, the precipitate was dissolved in a minimum amount of MeOH and purified via flash column chromatography ($SiO_2$, MeOH, $R_f$ = 0.74). The selected fractions containing the product were combined, and the solvent was removed under reduced pressure to give a dark purple solid, which was redissolved in DCM and filtered; the solvent was again removed, and then the product was dried overnight in a vacuum desiccator. Yield: 20.2 mg (20%).

*Synthesis of [Os(η⁶-p-cym)(N,C-AZBTZ-NMe₂)I] (**3b**).* $[Os(\eta^6\text{-}p\text{-cym})I_2]_2$ (50.0 mg, 43.2 μmol) and 4-(2-benzothiazolylazo)-*N,N*-dimethylaniline (24.4 mg, 86.5 μmol) were dissolved in EtOH (20 mL). The mixture was stirred at 50 °C for 2 h while the color changed to dark blue-purple. It was then stirred for 18 h at ambient temperature, at which point the volume was reduced under reduced pressure to ∼2 mL. The mixture was placed in a freezer (−20 °C) overnight, resulting in a dark brown precipitate, which was collected by filtration and washed with ice-cold EtOH (2 × 1 mL) and $Et_2O$ (2 × 5 mL). The product was dried overnight in a vacuum desiccator. Yield: 48.6 mg (77%).

*Synthesis of [Os(η⁶-p-cym)(N,N-AZBTZ*-NH₂)Cl]PF₆ (**4**).* $[Os(\eta^6\text{-}p\text{-cym})Cl_2]_2$ (30.0 mg, 37.9 μmol) was stirred in EtOH (10 mL), and a solution of *p*-(2-benzothiazolylazo)-3,5-dimethylaniline (22.5 mg, 79.7 μmol) in EtOH (5 mL) was added dropwise to the stirred mixture. The mixture was stirred for 2 h at 50 °C, and the color changed to dark blue-purple. The mixture was then stirred for 18 h at ambient temperature, and then $NH_4PF_6$ (61.8 mg, 0.38 mmol) was added. The mixture was concentrated under reduced pressure and placed in a freezer (−20 °C) overnight. The resulting dark purple precipitate was collected by filtration and washed with ice-cold EtOH (2 × 1 mL) and $Et_2O$ (2 × 5 mL). The product was dried overnight in a vacuum desiccator. Yield: 41.0 mg (69%).

*Synthesis of [Os(η⁶-p-cym)(N,N-AZBTZ*-NH₂)I]PF₆ (**5**).* $[Os(\eta^6\text{-}p\text{-cym})I_2]_2$ (23.1 mg, 20.0 μmol) was stirred in EtOH (10 mL), and a solution of *p*-(2-benzothiazolylazo)-3,5-dimethylaniline (11.3 mg, 39.9 μmol) in EtOH (5 mL) was added dropwise to the stirred mixture. The mixture was stirred for 2 h at 50 °C, and the color changed to dark blue-purple. The mixture was stirred for 18 h at ambient temperature, and then $NH_4PF_6$ (32.6 mg, 0.20 mmol) was added. The mixture was concentrated under reduced pressure and placed in a freezer (−20 °C) overnight. The resulting dark purple precipitate was collected by filtration and washed with ice-cold EtOH (2 × 1 mL) and $Et_2O$ (2 × 5 mL). The product was dried overnight in a vacuum desiccator. Yield: 20.4 mg (58%).

**Methods and Instrumentation.** *X-ray Crystallography.* Diffraction data were collected on an Oxford Diffraction Gemini four-circle system with a Ruby CCD area detector. All structures were refined by full-matrix least squares against $F^2$ using SHELXL 97 and were solved by direct methods using SHELXS(TREF) with additional light atoms found by Fourier methods. Hydrogen atoms were added at calculated positions and refined using a riding model. Anisotropic displacement parameters were used for all non-H atoms; H atoms were given an isotropic displacement parameter equal to 1.2 (or 1.5 for methyl and NH H atoms) times the equivalent isotropic displacement parameter of the atom to which they are attached. The data were processed by the modeling program Mercury 1.4.1.

X-ray crystallographic data for complexes **1a**, **2a**, **2b**·0.5$C_3H_6O$, and **3b**·0.5$CHCl_3$ have been deposited with the Cambridge Crystallographic Data Centre under the accession numbers CCDC 1540385−1540388, respectively.

*NMR Spectroscopy.* $^1H$ NMR and $^{13}C$ NMR spectra were acquired in 5 mm NMR tubes at 25 °C on Bruker DPX-400, HD-500, AV-600, and AV-700 spectrometers. Data processing was carried out using TOPSPIN version 2.1 (Bruker U.K. Ltd.). $^1H$ NMR chemical shifts were internally referenced to TMS via their residual solvent peaks with acetonitrile (δ 1.94 ppm), acetone (δ 2.05 ppm), methanol (δ 3.31 ppm), chloroform (δ 7.26 ppm), and DMSO (δ 2.50 ppm), and similarly for $^{13}C$ NMR chemical shifts with acetonitrile (δ 118.26 ppm). $^1H$ NMR spectra were recorded using standard pulse sequences, and $^{13}C$ NMR spectra were recorded using a JMOD pulse sequence.



DOI: 10.1021/acs.organomet.7b00501
Organometallics 2017, 36, 4367−4375

The 1D $^1$H sel-NOE NMR experiment was conducted using an AV-600 instrument, on irradiation of the $^1$H resonance at 6.84 ppm.

*Mass Spectrometry.* Electrospray mass spectra were obtained using the Agilent 6130B single Quad (ESI) mass spectrometer. Samples of complexes were typically prepared in methanol or acetonitrile and run in positive ion mode ($m/z$ 500−1000). Likewise, the analysis of the sample submitted for high-resolution mass spectroscopy was carried out using a Bruker MaXis UHR-ESI-TOF instrument.

*Elemental Analysis.* All purified complexes and ligands were analyzed via elemental analysis. Analyses (carbon, hydrogen, and nitrogen) were performed by Warwick Analytical Service using an Exeter Analytical elemental analyzer (CE440).

*Stability Study of **2b** under Acidic Conditions.* Solutions of complex **2b** (1.13 mg, 1.648 μmol) in methanol-$d_4$ (700 μL), and 0.889 M HBr in methanol-$d_4$ were prepared. HBr (9.27 μL, 5 mol equiv) was combined with the complex, and a 400 MHz $^1$H NMR spectrum was recorded every 30 min for 16 h at 25 °C.

*Aqueous Solution Chemistry.* Solutions of complexes **1a**,**b** were prepared in $H_2O$/MeOH (1/1, v/v) at a concentration of 50 μM. The UV−vis spectrum was measured at 25 °C every 1 h for 24 h on a Varian Cary 300 Bio instrument. Also measured was a 50 μM solution of complex **1a** in $H_2O$/MeOH (1/1, v/v) with 100 mM NaCl.

*Calculation of Partial Charges.* The Mulliken partial charges of complex **2b** were calculated for the optimized gas phase geometry, using the Gaussian 03 program and employing the DFT method and PBE1PBE functionals. A LanL2DZ basis set and effective core potential was used for the osmium atom, and a 6-31G**+ basis set was used for all other atoms.

## ■ ASSOCIATED CONTENT

### Supporting Information

The Supporting Information is available free of charge on the ACS Publications website at DOI: 10.1021/acs.organomet.7b00501.

Experimental data on the synthesis and characterization of complexes and ligands, crystallographic data, reaction schemes and proposed reaction mechanisms, additional NMR spectra, X-ray crystal structures, and UV−vis, MS, and kinetic data (PDF)

### Accession Codes

CCDC 1540385−1540388 contain the supplementary crystallographic data for this paper. These data can be obtained free of charge via www.ccdc.cam.ac.uk/data_request/cif, or by emailing data_request@ccdc.cam.ac.uk, or by contacting The Cambridge Crystallographic Data Centre, 12 Union Road, Cambridge CB2 1EZ, UK; fax: +44 1223 336033.

## ■ AUTHOR INFORMATION


### Corresponding Author

*E-mail for P.J.S.: e-mail, P.J.Sadler@Warwick.ac.uk; tel, +44 24 765 23818.

### ORCID

Nicolas P. E. Barry: 0000-0002-0388-6295

Peter J. Sadler: 0000-0001-9160-1941


### Notes

The authors declare no competing financial interest.

## ■ ACKNOWLEDGMENTS

We thank the ERC (Grant No. 247450), EPSRC (Grant No. EP/F034210/1), and The Royal Society (University Research Fellowship No. UF150295 to N.P.E.B.) for financial support, Dr. Ivan Prokes for NMR technical support, and Phil Aston for collecting high-resolution ESI mass spectra.

## ■ REFERENCES


(1) Coverdale, J. P. C.; Sanchez-Cano, C.; Clarkson, G. J.; Soni, R.; Wills, M.; Sadler, P. J. *Chem. - Eur. J.* **2015**, *21*, 8043−8046.

(2) Shul'pin, G. B.; Kozlov, Y. N.; Shul'pina, L. S.; Kudinov, A. R.; Mandelli, D. *Inorg. Chem.* **2009**, *48*, 10480−10482.

(3) Bertoli, M.; Choualeb, A.; Lough, A. J.; Moore, B.; Spasyuk, D.; Gusev, D. G. *Organometallics* **2011**, *30*, 3479−3482.

(4) Castarlenas, R.; Esteruelas, M. A.; Oñate, E. *Organometallics* **2005**, *24*, 4343−4346.

(5) Hanif, M.; Babak, M. V.; Hartinger, C. G. *Drug Discovery Today* **2014**, *19*, 1640−1648.

(6) Pizarro, A.; Habtemariam, A.; Sadler, P. *Top. Organomet. Chem.* **2010**, *32*, 21−56.

(7) Cebrián-Losantos, B.; Krokhin, A. A.; Stepanenko, I. N.; Eichinger, R.; Jakupec, M. A.; Arion, V. B.; Keppler, B. K. *Inorg. Chem.* **2007**, *46*, 5023−5033.

(8) Büchel, G. E.; Stepanenko, I. N.; Hejl, M.; Jakupec, M. A.; Keppler, B. K.; Arion, V. B. *Inorg. Chem.* **2011**, *50*, 7690−7697.

(9) Ni, W. X.; Man, W. L.; Yiu, S. M.; Ho, M.; Cheung, M. T. W.; Ko, C. C.; Che, C. M.; Lam, Y. W.; Lau, T. C. *Chem. Sci.* **2012**, *3*, 1582−1588.

(10) Fu, Y.; Habtemariam, A.; Basri, A. M. B. H.; Braddick, D.; Clarkson, G. J.; Sadler, P. J. *Dalton Trans.* **2011**, *40*, 10553−10562.

(11) Fu, Y.; Habtemariam, A.; Pizarro, A. M.; van Rijt, S. H.; Healey, D. J.; Cooper, P. A.; Shnyder, S. D.; Clarkson, G. J.; Sadler, P. J. *J. Med. Chem.* **2010**, *53*, 8192−8196.

(12) Hearn, J. M.; Romero-Canelón, I.; Munro, A. F.; Fu, Y.; Pizarro, A. M.; Garnett, M. J.; McDermott, U.; Carragher, N. O.; Sadler, P. J. *Proc. Natl. Acad. Sci. U. S. A.* **2015**, *112*, E3800−E3805.

(13) Shnyder, S. D.; Fu, Y.; Habtemariam, A.; van Rijt, S. H.; Cooper, P. A.; Loadman, P. M.; Sadler, P. J. *MedChemComm* **2011**, *2*, 666−668.

(14) Romero-Canelón, I.; Mos, M.; Sadler, P. J. *J. Med. Chem.* **2015**, *58*, 7874−7880.

(15) Wang, M.; Funabiki, K.; Matsui, M. *Dyes Pigm.* **2003**, *57*, 77−86.

(16) Matsumura, K.; Ono, M.; Hayashi, S.; Kimura, H.; Okamoto, Y.; Ihara, M.; Takahashi, R.; Mori, H.; Saji, H. *MedChemComm* **2011**, *2*, 596−600.

(17) Shi, D. F.; Bradshaw, T. D.; Wrigley, S.; McCall, C. J.; Lelieveld, P.; Fichtner, I.; Stevens, M. F. G. *J. Med. Chem.* **1996**, *39*, 3375−3384.

(18) Chua, M. S.; Shi, D. F.; Wrigley, S.; Bradshaw, T. D.; Hutchinson, I.; Shaw, P. N.; Barrett, D. A.; Stanley, L. A.; Stevens, M. F. G. *J. Med. Chem.* **1999**, *42*, 381−392.

(19) Hutchinson, I.; Jennings, S. A.; Vishnuvajjala, B. R.; Westwell, A. D.; Stevens, M. F. G. *J. Med. Chem.* **2002**, *45*, 744−747.

(20) Mortimer, C. G.; Wells, G.; Crochard, J. P.; Stone, E. L.; Bradshaw, T. D.; Stevens, M. F. G.; Westwell, A. D. *J. Med. Chem.* **2006**, *49*, 179−185.

(21) Hussein, B. H. M.; Azab, H. A.; El-Azab, M. F.; El-Falouji, A. I. *Eur. J. Med. Chem.* **2012**, *51*, 99−109.

(22) Ginzinger, W.; Mühlgassner, G.; Arion, V. B.; Jakupec, M. A.; Roller, A.; Galanski, M.; Reithofer, M.; Berger, W.; Keppler, B. K. *J. Med. Chem.* **2012**, *55*, 3398−3413.

(23) Spillane, C. B.; Dabo, M. N. V.; Fletcher, N. C.; Morgan, J. L.; Keene, F. R.; Haq, I.; Buurma, N. J. *J. Inorg. Biochem.* **2008**, *102*, 673−683.

(24) Oi, S.; Fukita, S.; Hirata, N.; Watanuki, N.; Miyano, S.; Inoue, Y. *Org. Lett.* **2001**, *3*, 2579−2581.

(25) Ryabov, A. D.; Soukharev, V. S.; Alexandrova, L.; Le Lagadec, R.; Pfeffer, M. *Inorg. Chem.* **2003**, *42*, 6598−6600.

(26) Davies, D. L.; Donald, S. M. A.; Al-Duaij, O.; Macgregor, S. A.; Pölleth, M. *J. Am. Chem. Soc.* **2006**, *128*, 4210−4211.

(27) Boutadla, Y.; Al-Duaij, O.; Davies, D. L.; Griffith, G. A.; Singh, K. *Organometallics* **2009**, *28*, 433−440.

(28) Li, B.; Roisnel, T.; Darcel, C.; Dixneuf, P. H. *Dalton Trans.* **2012**, *41*, 10934−10937.

(29) Abbenhuis, H. C. L.; Pfeffer, M.; Sutter, J. P.; de Cian, A.; Fischer, J.; Ji, H. L.; Nelson, J. H. *Organometallics* **1993**, *12*, 4464−4472.




DOI: 10.1021/acs.organomet.7b00501
*Organometallics* 2017, 36, 4367−4375

(30) Clark, A. M.; Rickard, C. E. F.; Roper, W. R.; Wright, L. J. *Organometallics* **1999**, *18*, 2813−2820.
(31) Fernandez, S.; Pfeffer, M.; Ritleng, V.; Sirlin, C. *Organometallics* **1999**, *18*, 2390−2394.
(32) Djukic, J.-P.; Berger, A.; Duquenne, M.; Pfeffer, M.; de Cian, A.; Kyritsakas-Gruber, N.; Vachon, J.; Lacour, J. *Organometallics* **2004**, *23*, 5757−5767.
(33) Cerón-Camacho, R.; Morales-Morales, D.; Hernandez, S.; Le Lagadec, R.; Ryabov, A. D. *Inorg. Chem.* **2008**, *47*, 4988−4995.
(34) Ferrer Flegeau, E.; Bruneau, C.; Dixneuf, P. H.; Jutand, A. *J. Am. Chem. Soc.* **2011**, *133*, 10161−10170.
(35) Ackermann, L. *Chem. Rev.* **2011**, *111*, 1315−1345.
(36) Baya, M.; Eguillor, B.; Esteruelas, M. A.; Lledós, A.; Oliván, M.; Oñate, E. *Organometallics* **2007**, *26*, 5140−5152.
(37) Zhang, Z.; Di, D.; Zhai, J.; Wu, L.; Zhu, Q.; Xu, Y.; Huang, R. *Chem. Res. Chin. Univ.* **2014**, *30*, 185−189.
(38) Cabeza, J. A.; Maitlis, P. M. *J. Chem. Soc., Dalton Trans.* **1985**, 573−578.
(39) Peacock, A. F. A.; Habtemariam, A.; Fernández, R.; Walland, V.; Fabbiani, F. P. A.; Parsons, S.; Aird, R. E.; Jodrell, D. I.; Sadler, P. J. *J. Am. Chem. Soc.* **2006**, *128*, 1739−1748.
(40) Clayton, H. S.; Makhubela, B. C. E.; Su, H.; Smith, G. S.; Moss, J. R. *Polyhedron* **2009**, *28*, 1511−1517.



DOI: 10.1021/acs.organomet.7b00501
*Organometallics* 2017, 36, 4367−4375

# Halide Control of *N,N*-Coordination versus *N,C*-Cyclometallation and Stereospecific Phenyl Ring Deuteration of Osmium(II) *p*-Cymene Phenylazobenzothiazole Complexes.

Russell J. Needham, Abraha Habtemariam, Nicolas P. E. Barry, Guy Clarkson, and Peter J. Sadler

## Supporting Information

# Experimental

## Synthesis and characterization of ligands and complexes

**4-(2-Benzothiazolylazo)-*N,N*-dimethylaniline (L).** Yield: 585.6 mg, (62%). $^1$H NMR (400 MHz, $CDCl_3$): δ 8.07 (d, 1H, J = 7.8 Hz), 8.00 (d, 2H, J = 9.1 Hz), 7.84 (d, 1H, J = 7.8 Hz), 7.47-7.46 (m, 1H), 7.38-7.37 (m, 1H), 6.77 (d, 2H, J = 9.4 Hz), 3.17 (s, 6H). ESI-MS calculated for $C_{15}H_{14}N_4S + H^+$: m/z 283.1. Found: 283.1. CHN analysis: Found: C, 63.22%; H, 4.92%; N, 19.67%. Calculated for $C_{15}H_{14}N_4S$: C, 63.81%; H, 5.00%; N, 19.84%.

***para*-(2-Benzothiazolylazo)-3,5-dimethylaniline (L*).** The crude product was purified *via* flash column chromatography ($SiO_2$, 1:2 acetone:*n*-hexane, $R_f$ = 0.33). Due to low solubility of the crude product in the mobile phase, it was possible to purify only a portion of the crude product. The collected fractions containing product were combined and the solvent was removed under reduced pressure to yield a dark red precipitate, which was dried overnight in a vacuum desiccator. Yield: 53.2 mg. $^1$H NMR (400 MHz, $CDCl_3$): δ 8.08 (d, 1H, J = 8.0 Hz), 7.81 (d, 1H, J = 8.0 Hz), 7.46-7.45 (m, 1H), 7.37-7.36 (m, 1H), 6.43 (s, 2H), 4.33 (s. br, 2H), 2.64 (s, 6H). ESI-MS calculated for $C_{15}H_{14}N_4S + H^+$: m/z 283.1. Found: 282.8.CHN analysis: Found: C, 63.35%; H, 5.00%; N, 19.60%. Calculated for $C_{15}H_{14}N_4S$: C, 63.81%; H, 5.00%; N, 19.84%.

**[Os(η$^6$-*p*-cym)(*N,N*-AZBTZ-NMe$_2$)Cl]PF$_6$ (1a).** $^1$H NMR (400 MHz, $CD_3OD$): δ 8.28-8.27 (m, 2H), 8.15-8.14 (m, 2H), 7.83-7.82 (m, 1H), 7.75-7.74 (m, 1H), 7.06-7.05 (m, 2H), 6.59-6.58 (m, 1H), 6.55-6.54 (m, 1H), 6.25-6.24 (m, 1H), 6.21-6.20 (m, 1H), 3.53 (s, 6H), 2.48 (s, 3H), 2.18 (sept., 1H, J = 6.9 Hz), 0.87 (d, 3H, J = 6.9 Hz), 0.76 (d, 3H, J = 6.9 Hz). ESI-MS calculated for $C_{25}H_{28}ClN_4OsS^+$: m/z 643.1. Found: 643.0. CHN analysis: Found: C, 38.30%; H, 3.46%; N, 6.95%. Calculated for $C_{25}H_{28}ClF_6N_4OsPS$: C, 38.14%; H, 3.59%; N, 7.12%.

**Os(η$^6$-*p*-cym)(*N*,*C*-AZBTZ-NMe$_2$)Cl (1b).** $^1$H NMR (400 MHz, $(CD_3)_2CO$): δ 8.10 (m, 1H), 8.08 (d, 1H, J = 9.4 Hz), 7.96-7.95 (m, 1H), 7.60-7.59 (m, 2H), 7.47-7.46 (m, 1H), 6.94 (dd, 1H, J = 9.4, 2.7 Hz), 6.24-6.23 (m, 1H), 6.14-6.13 (m, 1H), 6.03-6.02 (m, 1H), 5.46-5.45 (m, 1H), 3.45 (s, 6H), 2.32 (sept., 1H, J = 6.9 Hz), 2.25 (s, 3H), 1.04 (d, 3H, J = 6.9 Hz), 0.79 (d, 3H, J = 6.9 Hz). ESI-MS calculated for $C_{25}H_{27}ClN_4OsS + H^+$: m/z 643.1. Found: 643.0. CHN analysis: Found: C, 46.67%; H, 4.39%; N, 8.34%. Calculated for $C_{25}H_{27}ClN_4OsS$: C, 46.83%; H, 4.24%; N, 8.74%.

**[Os(η$^6$-*p*-cym)(*N*,*N*-AZBTZ-NMe$_2$)Br]PF$_6$ (2a).** $^1$H NMR (400 MHz, $(CD_3)_2CO$): δ 8.36 (d, 2H, J = 9.6 Hz), 8.23-8.22 (m, 2H), 7.80-7.79 (m, 2H), 7.07 (d, 2H, J = 9.7 Hz), 6.80-6.79 (m, 1H), 6.75-6.74 (m, 1H), 6.46-6.45 (m, 1H), 6.41-6.40 (m, 1H), 3.58 (s, 6H), 2.66 (s, 3H), 2.26 (sept., 1H, J = 6.9 Hz), 0.94 (d, 3H, J = 6.9 Hz), 0.85 (d, 3H, J = 6.9 Hz). ESI-MS calculated for $C_{25}H_{28}BrN_4OsS^+$: m/z 687.1. Found: 687.1. No CHN analysis obtained due to low yield, but a crystal suitable for structure determination by x-ray crystallography was obtained (*vide infra*).

**Os(η$^6$-*p*-cym)(*N*,*C*-AZBTZ-NMe$_2$)Br (2b).** $^1$H NMR (400 MHz, $(CD_3)_2SO$): δ 7.98-7.91 (m, 1H), 7.96 (d, 1H, J = 9.3 Hz), 7.48-7.47 (m, 1H), 7.43 (d, 1H, J = 2.6 Hz), 7.35-7.34 (m, 1H), 6.85 (dd, 1H, J = 9.3, 2.6 Hz), 6.15-6.14 (m, 2H), 5.81-5.80 (m, 1H), 5.49-5.48 (m, 1H), 3.34 (s, 6H, *hidden under water peak*), 2.31 (sept., 1H, J = 6.9 Hz), 2.16 (s, 3H), 0.99 (d, 3H, J = 6.9 Hz), 0.70 (d, 3H, J = 6.9 Hz). $^{13}$C NMR (500 MHz, $CD_3CN$): δ 186.48 (*C*), 175.49 (*C*), 157.00 (*C*), 153.32 (*C*), 152.59 (*C*), 135.27 (*C*), 133.35 (*C*H), 127.06 (*C*H), 125.63 (*C*H), 123.46 (*C*H), 122.60 (*C*H), 120.51 (*C*H), 113.91 (*C*H), 100.28 (*C*), 95.79 (*C*), 87.41 (*C*H), 84.90 (*C*H), 77.08 (*C*H), 74.45 (*C*H), 40.86 (*C*H$_3$), 31.95 (*C*H), 23.17 (*C*H$_3$), 21.85 (*C*H$_3$), 19.65 (*C*H$_3$). ESI-MS calculated for $C_{25}H_{27}BrN_4OsS + H^+$ and $C_{25}H_{27}BrN_4OsS + Na^+$: m/z 687.1 and 709.1. Found: 687.0 and 708.9. CHN analysis: Found: C, 42.68%; H, 3.84%; N, 8.00 %. Calculated for $C_{25}H_{27}BrN_4OsS + \frac{1}{3}CH_2Cl_2$: C, 42.61%; H, 3.91%; N, 7.85%.

**Os(η$^6$-*p*-cym)(*N,C*-AZBTZ-NMe$_2$)I (3b).** $^1$H NMR (700 MHz, $CDCl_3$): δ 8.11 (d, 1H, J = 9.2 Hz), 7.93 (d, 1H, J = 8.0 Hz), 7.76 (d, 1H, J = 7.9 Hz), 7.42-7.41 (m, 1H), 7.30-7.29 (m, 1H), 7.27 (d, 1H, J = 2.5 Hz), 6.71 (dd, 1H, J = 9.2, 2.5 Hz), 5.99-5.98 (m, 1H), 5.87-5.86 (m, 1H), 5.67-5.66 (m, 1H), 5.36-5.35 (m, 1H), 3.32 (s, 6H), 2.58 (sept., 1H, J = 6.9 Hz), 2.41 (s, 3H), 1.13 (d, 3H, 6.9 Hz), 0.83 (d, 3H, 6.9 Hz). ESI-MS calculated for $C_{25}H_{27}IN_4OsS + H^+$ and $C_{25}H_{27}IN_4OsS + Na^+$: m/z 735.1 and 757.1. Found: 735.0 and 756.9. CHN analysis: Found: C, 40.56%; H, 3.74%; N, 7.28%. Calculated for $C_{25}H_{27}IN_4OsS$: C, 40.98%; H, 3.71%; N, 7.65%.

**[Os(η$^6$-*p*-cym)(*N,N*-AZBTZ*-NH$_2$)Cl]PF$_6$ (4).** $^1$H NMR (400 MHz, $CDCl_3$): δ 8.22 (d, 1H, J = 8.3 Hz), 8.06-7.99 (m, 2H), 7.92-7.91 (m, 1H), 6.90-6.89 (m, 1H), 6.60-6.59 (m, 1H), 6.48-6.47 (m, 1H), 6.05-6.04 (m, 1H), 5.90-5.89 (m, 1H), 5.65-5.64 (m, 1H), 4.20 (s. br, 2H), 2.49 (s, 3H), 2.34 (s, 3H), 2.28 (sept., 1H, J = 6.9 Hz), 1.92 (s, 3H), 1.11 (d, 3H, J = 6.9 Hz), 0.91 (d, 3H, J = 6.9 Hz). $^{13}$C NMR (500 MHz, $CD_3CN$): δ 180.04 (*C*), 152.01 (*C*), 151.73 (*C*), 147.47 (*C*), 136.96 (*C*), 136.17 (*C*), 133.25 (*C*), 131.03 (*C*H), 130.34 (*C*H), 126.02 (*C*H), 124.03 (*C*H), 115.37 (*C*H), 114.13 (*C*H), 110.11 (*C*), 106.71 (*C*), 89.13 (*C*H), 86.71 (*C*H), 86.29 (*C*H), 85.46 (*C*H), 32.86 (*C*H), 23.02 (*C*H$_3$), 22.00 (*C*H$_3$), 20.47 (*C*H$_3$), 19.55 (*C*H$_3$), 19.13 (*C*H$_3$). ESI-MS calculated for $C_{25}H_{28}ClN_4OsS^+$: m/z 643.1. Found: 643.2.CHN analysis: Found: C, 38.14%; H, 3.59%; N, 7.12%. Calculated for $C_{25}H_{28}F_6ClN_4OsPS$: C, 37.54%; H, 3.46%; N, 7.13%.

**[Os(η$^6$-*p*-cym)(*N,N*-AZBTZ*-NH$_2$)I]PF$_6$ (5).** $^1$H NMR (400 MHz, $CDCl_3$): δ 8.22 (d, 1H, J = 8.3 Hz), 8.02-7.96 (m, 2H), 7.89-7.88 (m, 1H), 6.82-6.81 (m, 1H), 6.58-6.57 (m, 1H), 6.48-6.47 (m, 1H,), 6.08-6.07 (m, 1H), 5.94-5.93 (m, 1H), 5.74-5.73 (m, 1H), 4.13 (s. br, 2H), 2.69 (s, 3H), 2.62 (s, 3H), 2.53 (sept., 1H, J = 6.9 Hz), 1.86 (s, 3H), 1.05 (d, 3H, J = 6.9 Hz), 1.01 (d, 3H, J = 6.9 Hz). $^{13}$C NMR ($CD_3CN$): δ 179.35 (*C*), 152.80 (*C*), 151.23 (*C*), 148.86 (*C*), 135.58 (*C*), 135.24 (*C*), 132.70 (*C*), 130.81 (*C*H), 130.19 (*C*H), 126.10 (*C*H), 124.69 (*C*H),

115.08 (*C*H), 114.03 (*C*H), 109.74 (*C*), 103.72 (*C*), 90.64 (*C*H), 88.28 (*C*H), 87.16 (*C*H), 84.82 (*C*H), 33.42 (*C*H), 23.39 (*C*$H_3$), 22.65 (*C*$H_3$), 22.46 (*C*$H_3$), 20.89 (*C*$H_3$), 19.46 (*C*$H_3$). ESI-MS calculated for $C_{25}H_{28}IN_4OsS^+$: m/z 735.1. Found: 735.0.

**Crystal Growth.** Single crystals of **1a** and **2b** (as **2b**·0.5$C_3H_6O$), suitable for x-ray crystallography were obtained by diffusion of *n*-hexane into an acetone solution at ambient temperature. Crystals of **2a** were obtained by slow evaporation of a MeOH solution at ambient temperature. Crystals of **3b** (as **3b**·0.5$CHCl_3$) were obtained by slow evaporation of a chloroform solution at ambient temperature.

**Table S1.** Crystallographic data for complexes **1a**, **2a**, **2b·0.5C$_3$H$_6$O** and **3b·0.5CHCl$_3$**

| | **1a** | **2a** | **2b**·0.5C$_3$H$_6$O | **3b**·0.5CHCl$_3$ |
|---|---|---|---|---|
| Formula | $C_{25}H_{28}ClF_6N_4OsPS$ | $C_{25}H_{28}BrF_6N_4OsPS$ | $C_{25}H_{27}BrN_4OsS{\cdot}0.5C_3H_6O$ | $C_{25}H_{27}IN_4OsS{\cdot}0.5CHCl_3$ |
| Molar mass /g mol$^{-1}$ | 787.19 | 831.65 | 714.71 | 792.35 |
| Density /mg m$^{-3}$ | 1.869 | 2.011 | 1.876 | 2.023 |
| Crystal system | Monoclinic | Monoclinic | Monoclinic | Monoclinic |
| Crystal dimensions /mm | 0.20 x 0.16 x 0.10 | 0.20 x 0.16 x 0.12 | 0.55 x 0.30 x 0.15 | 0.40 x 0.10 x 0.01 |
| Space group | C2/c | P2(1)/c | P2(1)/c | P2(1)/c |
| Crystal character | purple block | blue block | black block | brown plate |
| *a*/Å | 15.13119(10) | 14.5016(3) | 8.6795(3) | 8.7460(4) |
| *b*/Å | 14.67057(10) | 8.02434(13) | 26.5519(10) | 26.6356(13) |
| *c*/Å | 25.80898(15) | 24.5307(5) | 11.6929(5) | 11.8522(6) |
| *α*/deg | 90 | 90 | 90 | 90 |
| *β*/deg | 102.3937(6) | 105.825(2) | 110.116(4) | 109.545(5) |
| *γ*/deg | 90 | 90 | 90 | 90 |
| *T*/K | 100 | 150 | 150 | 100 |
| *Z* | 8 | 4 | 4 | 4 |
| *R [F> 4σ(F)]* | 0.0252 | 0.0267 | 0.0555 | 0.0686 |
| $R_w$ | 0.0638 | 0.0635 | 0.0997 | 0.1790 |
| GOF | 1.115 | 1.032 | 1.260 | 1.108 |
| Δρ max and min /eÅ$^{-3}$ | 1.397 & -0.862 | 3.098 & -0.989 | 2.967 & -3.209 | 3.646 & -2.888 |

**Scheme S1.** Diazotisation coupling reactions for the synthesis of **L** and **L***. (a) Glacial acetic acid:water:concentrated $H_2SO_4$ (6:3:2), $NaNO_2$, 0°C. (b) *N*,*N*-Dimethylaniline, MeOH, 0 °C. (c) 3,5-Dimethylaniline, MeOH, 0 °C.

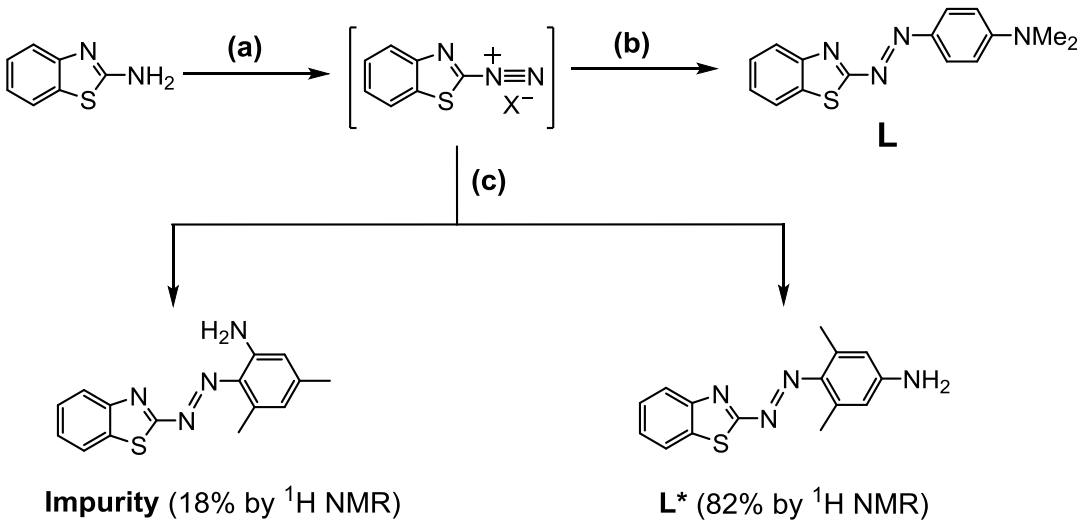


**Scheme S2.** Two possible mechanisms for ortho C-H bond deprotonation. (A) $S_E3$ mechanism. (B) An alternative mechanism involving an agnostic ortho Os(C-H) bond.

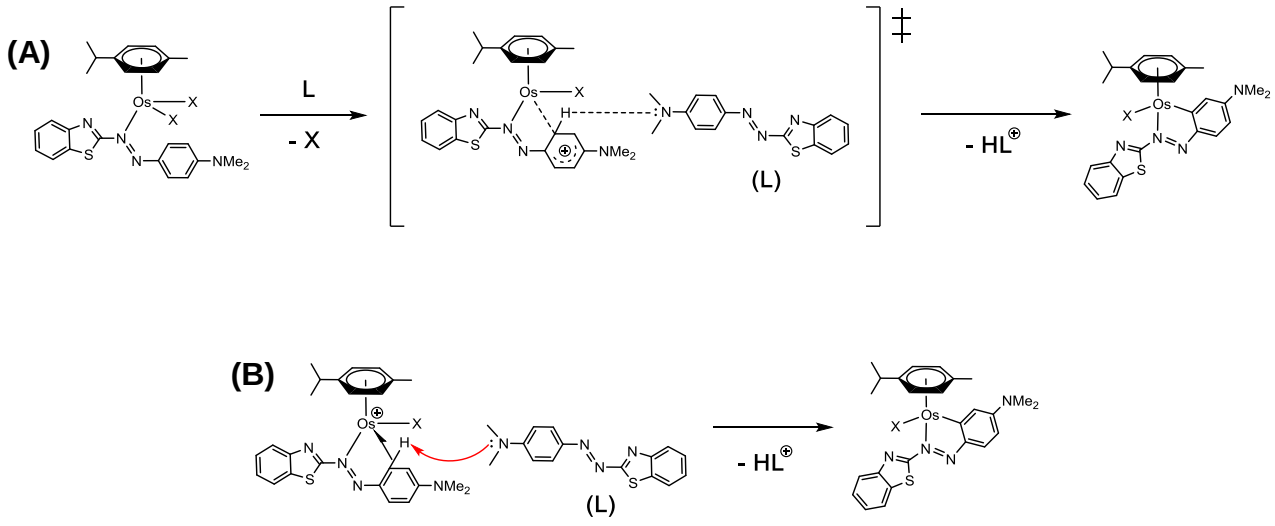

**Scheme S3.** Proposed mechanism for the associative exchange of $H_a$ with deuterium in complex **2b** under acidic conditions in methanol-*d*$_4$.

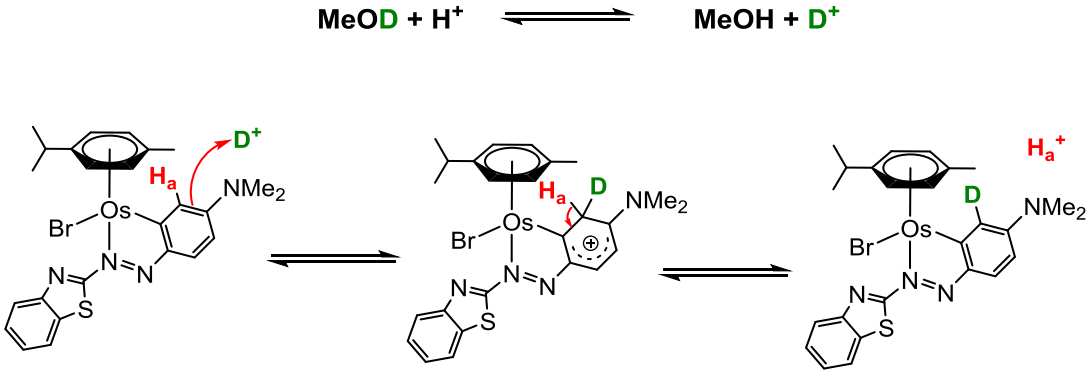

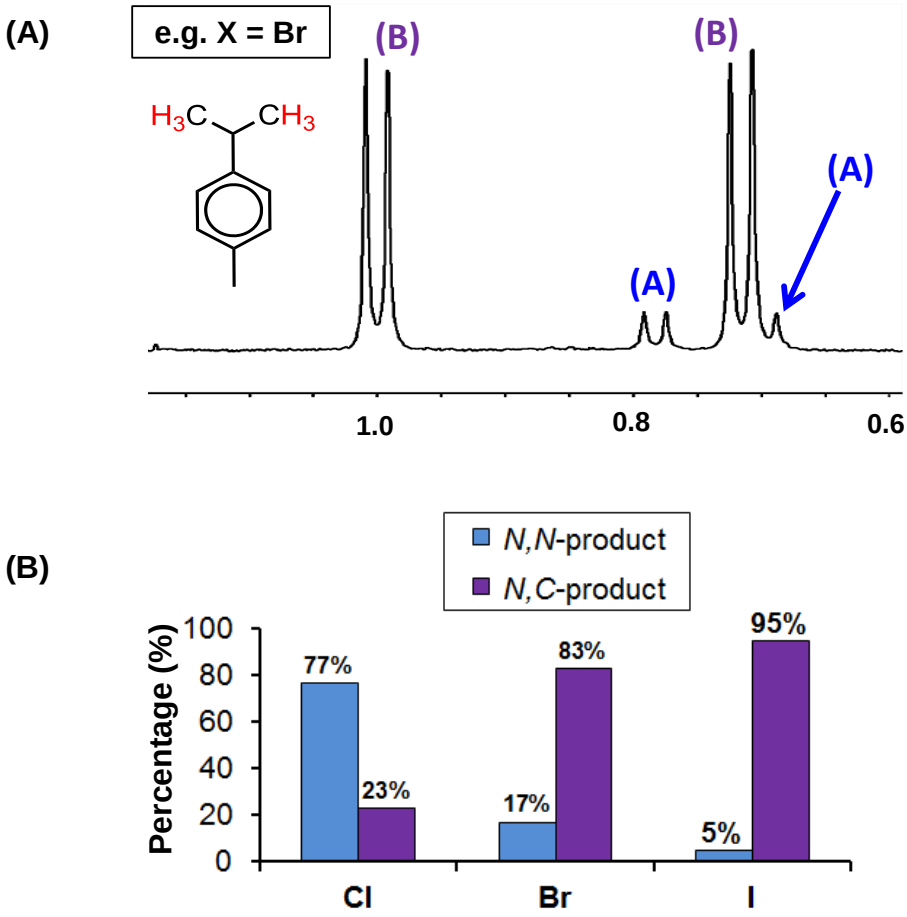


**Figure S1.** (A) The $^{1}$H NMR spectrum (aliphatic region, 400 MHz, DMSO-$d_6$) after a 18 h reaction of $[Os(\eta^6\text{-}p\text{-cym})Br_2]_2$ with **L**, showing two doublets for *p*-cym methyl groups of complexes **A** (*N*,*N*-coordination), and **B** (*N*,*C*-coordination). (B) The percentages of **A** and **B** formed when different dimers ($[Os(\eta^6\text{-}p\text{-cym})X_2]_2$, where X = Cl, Br or I) react with **L**.

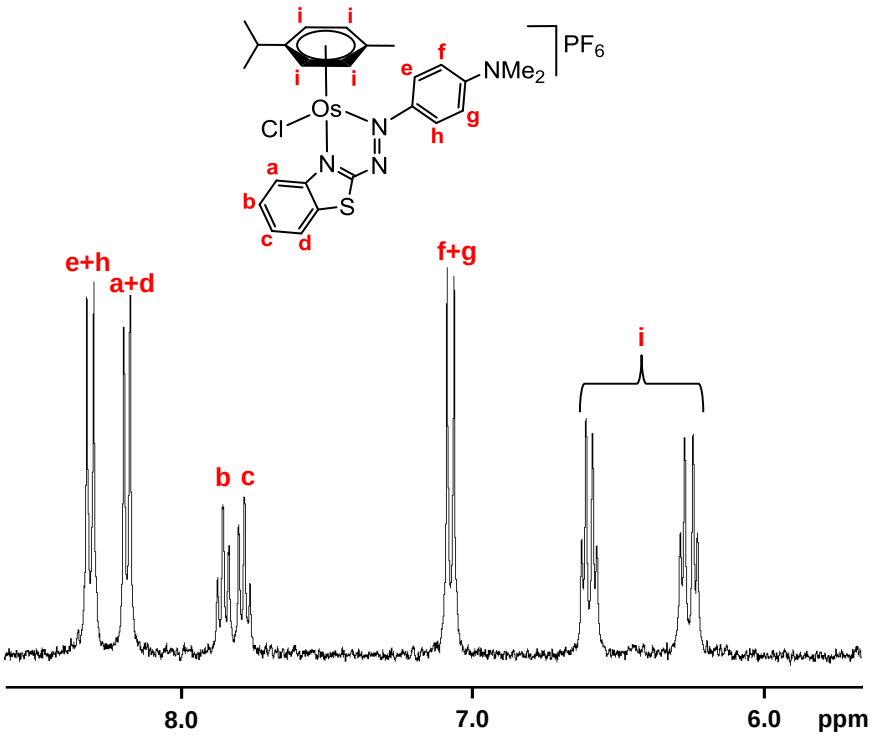


**Figure S2.** The aromatic region of the 400 MHz $^{1}$H NMR spectrum of complex **1a** in methanol-$d_4$, with assignments.

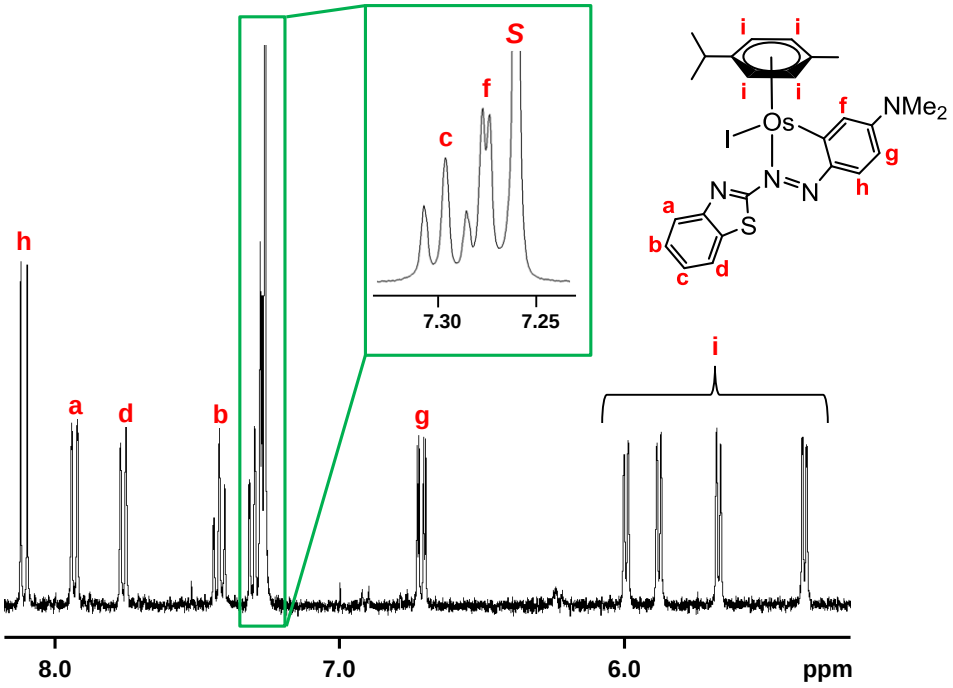


**Figure S3.** The aromatic region of the 700 MHz $^{1}$H NMR spectrum of complex **3b** in chloroform-$d_1$. The assignment of 11 aromatic protons is shown and residual solvent peak, *S*.

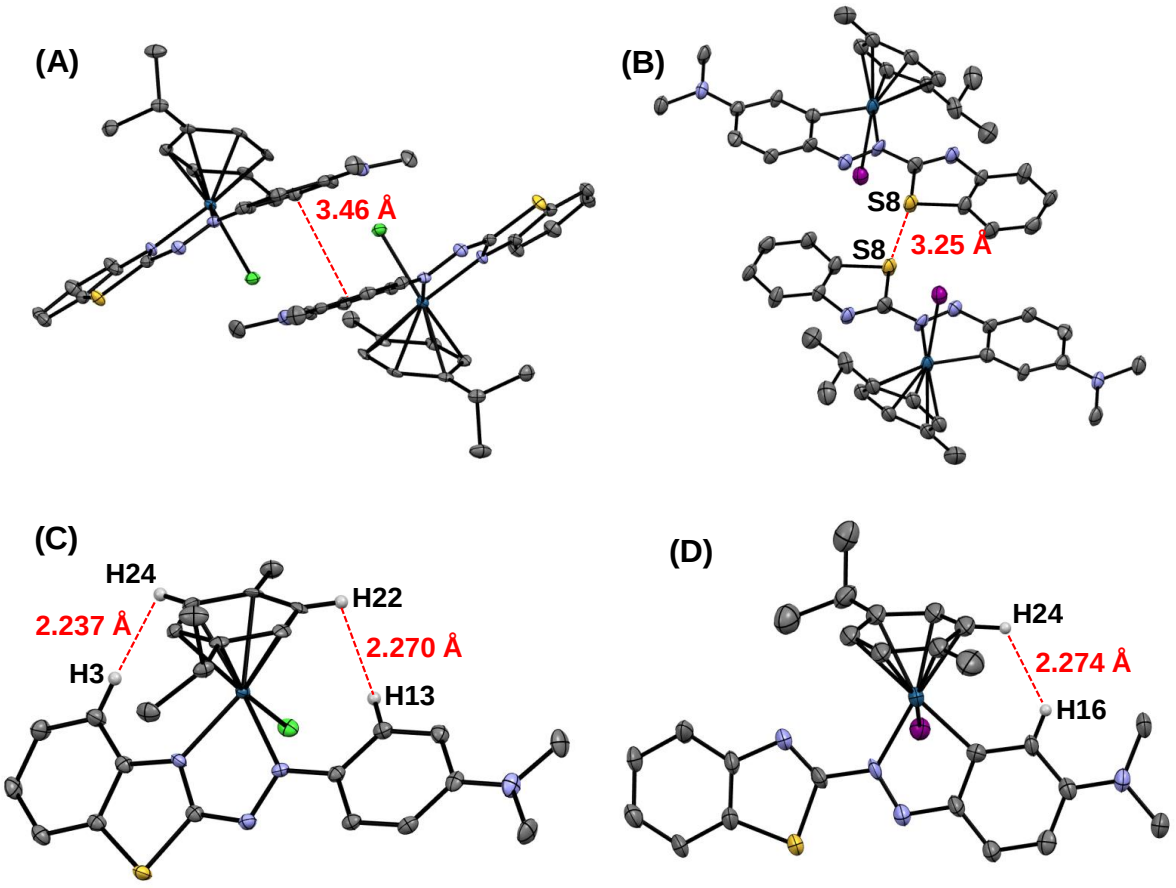


**Figure S4.** (A) Weak π-π interactions between aniline rings of complex **1a** (distances are centroid-to-centroid). (B) S···S bridging in complex **3b**·0.5$CHCl_3$. (C) H13···H22 and H3···H24 atom-atom distances in complex **1a**. (D) H16···H24 atom-atom distances in complex **3b**·0.5$CHCl_3$.

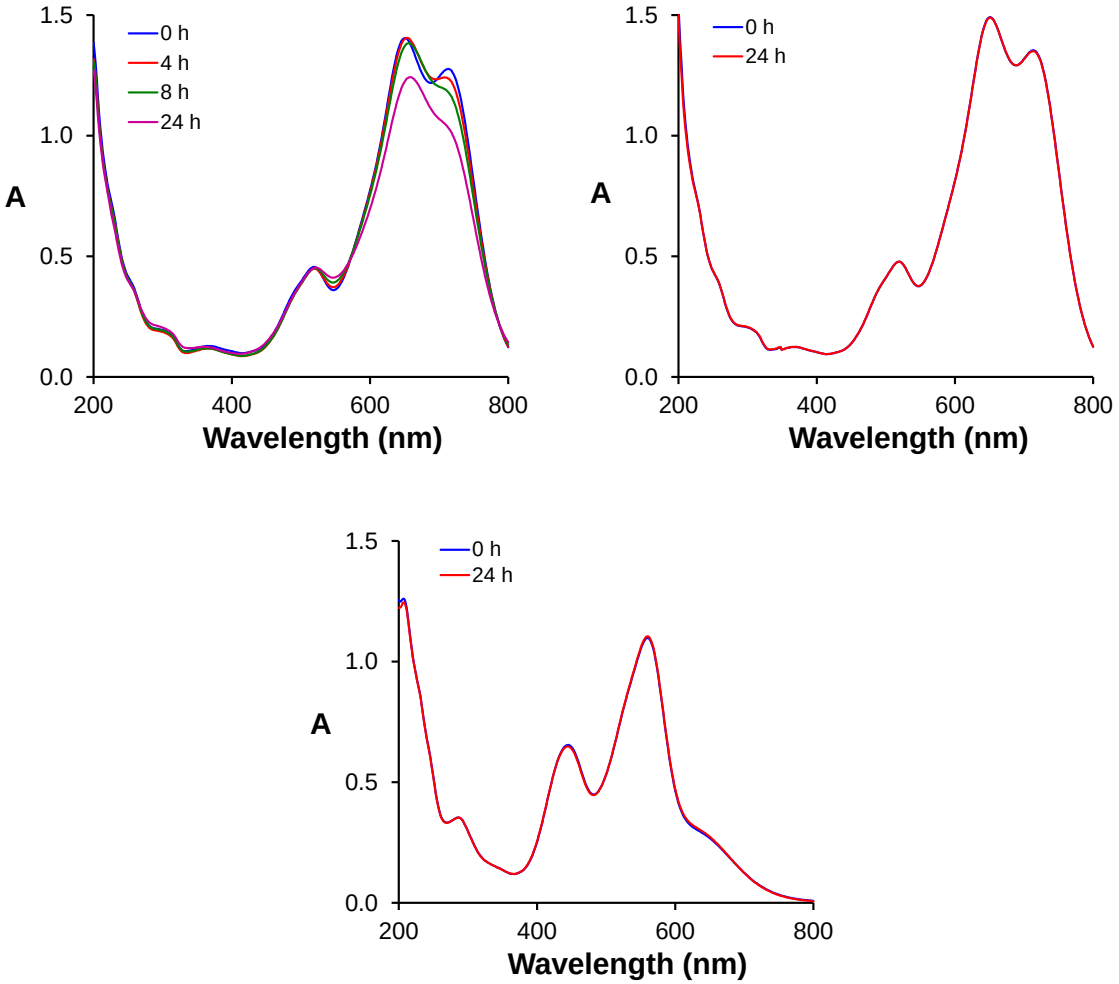


**Figure S5.** UV-Vis spectra of complexes in MeOH:$H_2O$ (1:1, v/v) at 25 °C. (A) 50 μM complex **1a**. (B) 50 μM complex **1a** with 100 mM NaCl. (C) 50 μM complex **3b**.

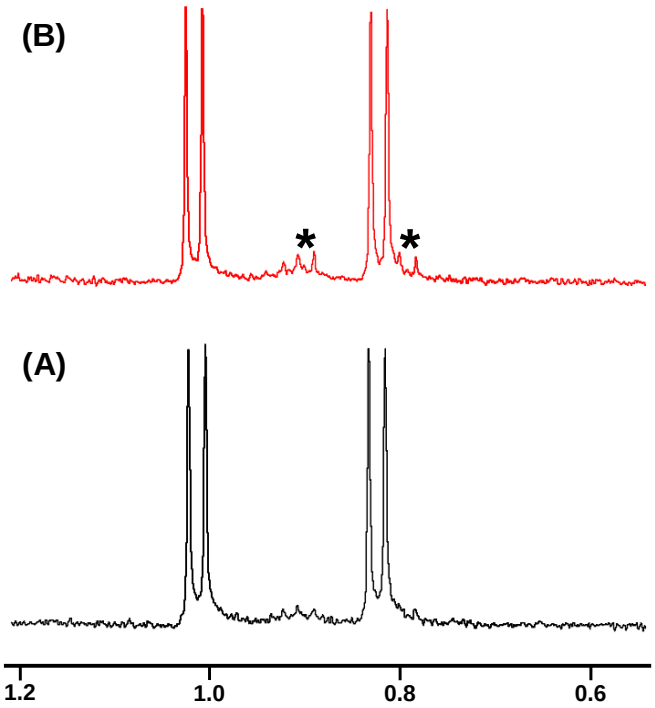


**Figure S6**. 400 MHz $^{1}$H NMR spectrum (aliphatic region) of the reaction mixture after heating *N*,*C*-coordinated complex **2b** under reflux in MeOH with HBr (100 mol equiv). (A) 1-day reflux, (B) 2-day reflux. A new set of small peaks is observed corresponding to an *N*,*N*-coordinated species, *.

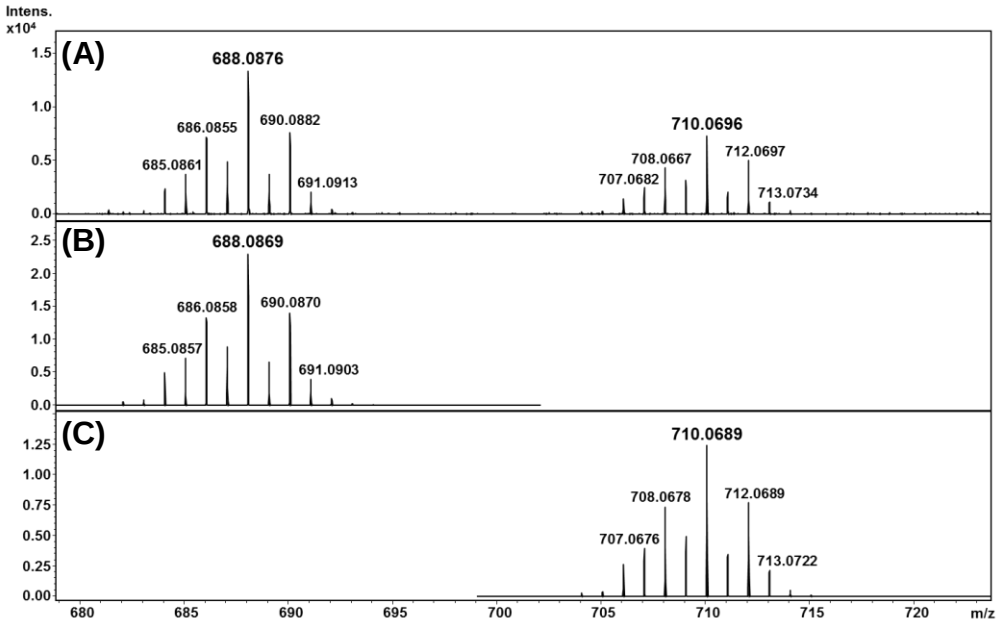


**Figure S7.** High resolution mass spectrum of complex **2b** after deuterium exchange of $H_a$. (A) Experimental spectrum, (B) calculated spectrum for $C_{25}H_{26}BrDN_4OsS + H^+$, (C) calculated spectrum for $C_{25}H_{26}BrDN_4OsS + Na^+$.

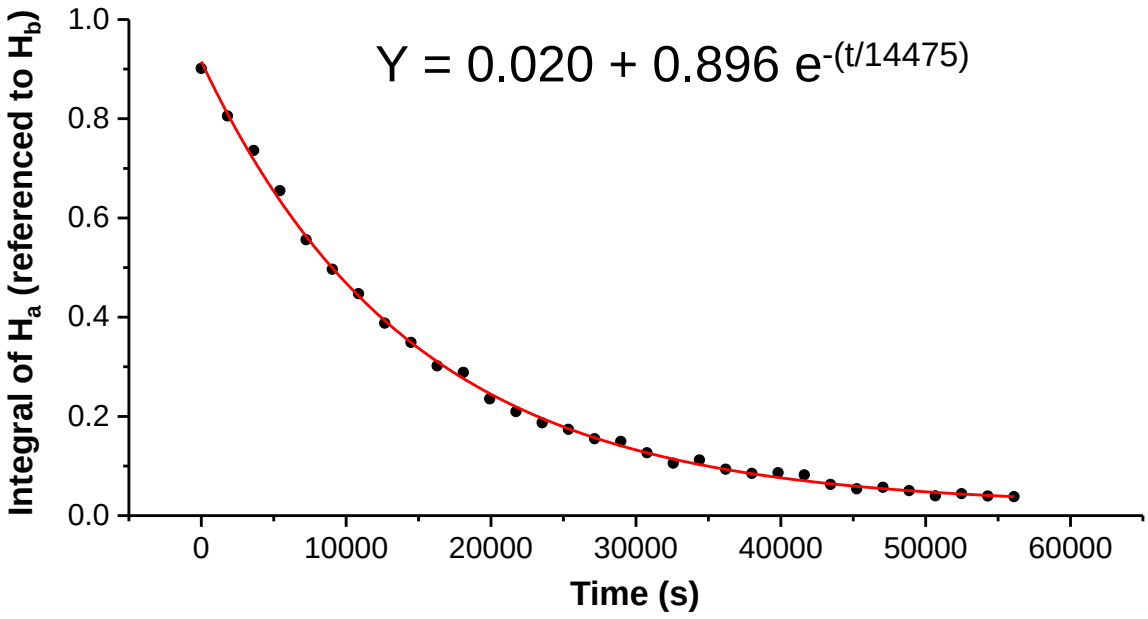


**Figure S8.** Time dependent disappearance of the NMR resonance, $H_a$ (7.58 ppm) in complex **2b** at 25 °C. $k$ = 6.91 x $10^{-5}$ $s^{-1}$ and $t_{1/2}$ = 1.00 x $10^4$ s.

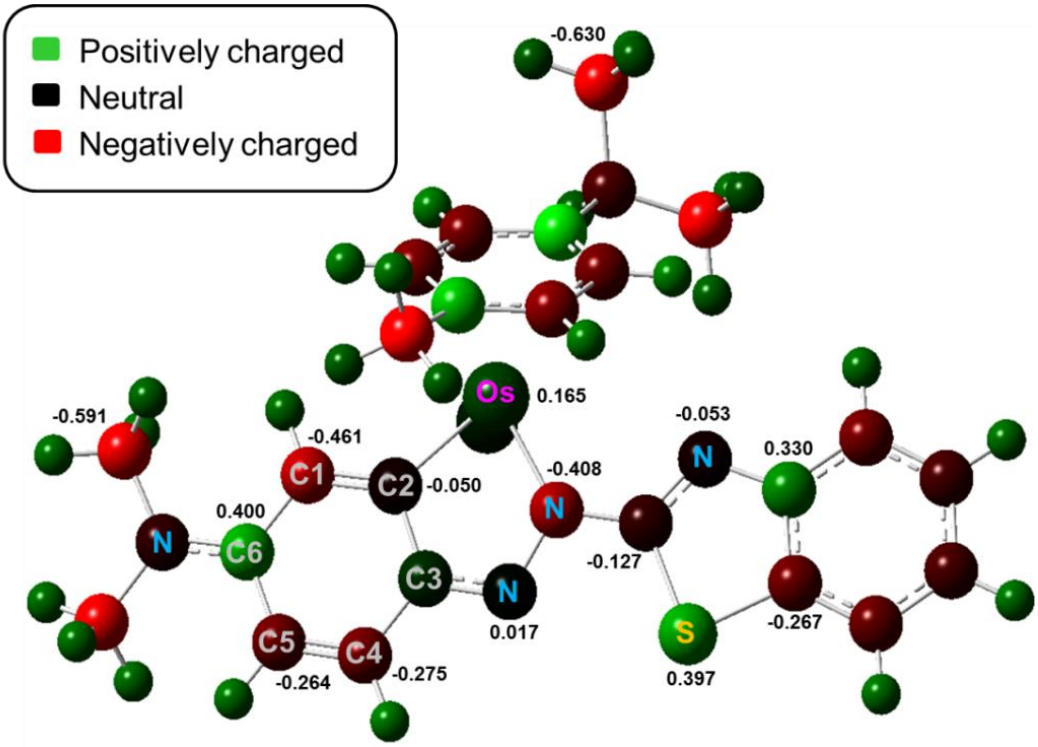


**Figure S9.** The Mulliken partial charges for complex **2b** showing the partial charges of selected atoms.